AD-A136 754 ELECTRON MICROSCOPY OF INTRACELLULAR PROTOZOA(U) CASE WESTERN RESERVE UNIV CLEVELAND OHIO INST OF PATHOLOGY M AIKAWA AUG 82 DAMD17-79-C-9029 1/2

UNCLASSIFIED F/G 6/5 NL

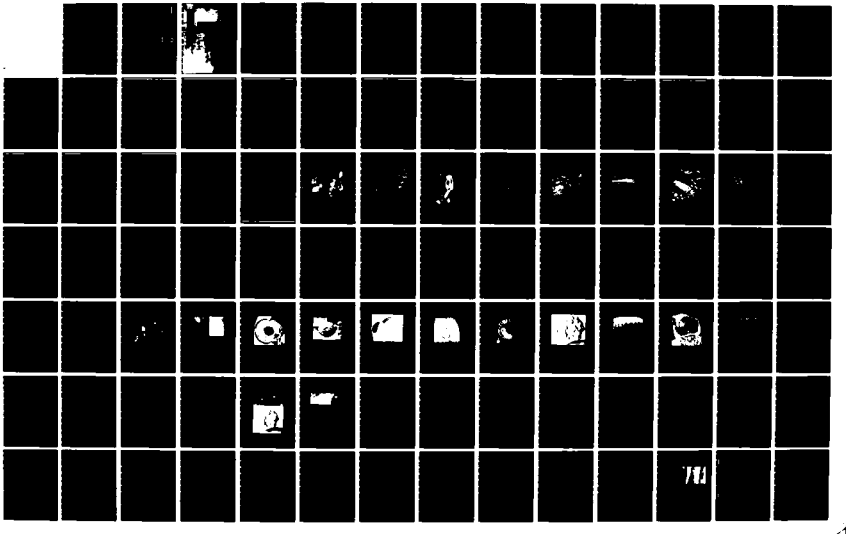

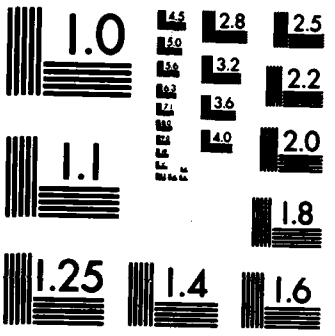

MICROCOPY RESOLUTION TEST CHART
NATIONAL BUREAU OF STANDARDS-1963-A

PHOTOGRAPH THIS SHEET

AD A136754

DTIC ACCESSION NUMBER

III

LEVEL

1

INVENTORY

Annual Rpt. #3, Aug. '82

DOCUMENT IDENTIFICATION

Aikawa, Masamichi
Contract DAMD17-79-C-9029

DISTRIBUTION STATEMENT A
Approved for public release;
Distribution Unlimited

A1

DISTRIBUTION STATEMENT

ACCESSION FOR	
NTIS	GRA&I
DTIC	TAB
UNANNOUNCED	
JUSTIFICATION	
BY	
DISTRIBUTION /	
AVAILABILITY CODES	
DIST	AVAIL AND/OR SPECIAL
A/1	

DISTRIBUTION STAMP

DTIC
ELECTE
JAN 12 1984
S D
D

DATE ACCESSIONED

DATE RETURNED

84 01 10 076

DATE RECEIVED IN DTIC

REGISTERED OR CERTIFIED NO.

PHOTOGRAPH THIS SHEET AND RETURN TO DTIC-DDAC

DTIC FORM 70A DEC 83

DOCUMENT PROCESSING SHEET

PREVIOUS EDITION MAY BE USED UNTIL STOCK IS EXHAUSTED.

ANNUAL REPORT #3

Electron Microscopy of Intracellular Protozoa

August, 1982

ELECTRON MICROSCOPY OF INTRACELLULAR PROTOZOA

Masamichi Aikawa, M.D.
August, 1982

Supported by

U. S. Army Medical Research and Development Command

Fort Detrick, Frederick, MD. 21701

Contract No. DAMD 17-79-C-9029

The Institute of Pathology

Case Western Reserve University

Cleveland, Ohio 44106

SECURITY CLASSIFICATION OF THIS PAGE (When Data Entered)

REPORT DOCUMENTATION PAGE		READ INSTRUCTIONS BEFORE COMPLETING FORM
1. REPORT NUMBER	2. GOVT ACCESSION NO.	3. RECIPIENT'S CATALOG NUMBER
4. TITLE (and Subtitle) Electron Microscopy of Intracellular Protozoa		5. TYPE OF REPORT & PERIOD COVERED Annual Report 6. PERFORMING ORG. REPORT NUMBER
7. AUTHOR(s) Masamichi Aikawa, M.D.		8. CONTRACT OR GRANT NUMBER(s) DAMD17-79-C-9029
9. PERFORMING ORGANIZATION NAME AND ADDRESS Case Western Reserve University Cleveland, Ohio 44106		10. PROGRAM ELEMENT, PROJECT, TASK AREA & WORK UNIT NUMBERS 61102A.3M161102BS10.AF.050
11. CONTROLLING OFFICE NAME AND ADDRESS U.S. Army Medical Research & Development Command, Fort Detrick, Frederick, MD 21701		12. REPORT DATE August, 1982 13. NUMBER OF PAGES 98
14. MONITORING AGENCY NAME & ADDRESS(if different from Controlling Office)		15. SECURITY CLASS. (of this report) Unclassified 15a. DECLASSIFICATION/DOWNGRADING SCHEDULE

16. DISTRIBUTION STATEMENT (of this Report)

Approved for public release; distribution unlimited.

17. DISTRIBUTION STATEMENT (of the abstract entered in Block 20, if different from Report)

18. SUPPLEMENTARY NOTES

19. KEY WORDS (Continue on reverse side if necessary and identify by block number)

20. ABSTRACT (Continue on reverse side if necessary and identify by block number)

Summary

During this fiscal year, in collaboration with Col. Hendricks and his associates we studied the interactions between macrophage-like cells (P388D) and Leishmania braziliensis in vitro under various conditions by light and electron microscopy. When P388D and L. braziliensis were incubated together for two minutes, 90% of the promastigotes were attached to P388D by the tip of the flagella. The P388D did not form pseudopods or aggregated micro-

DD FORM 1 JAN 73 1473 EDITION OF 1 NOV 65 IS OBSOLETE

SECURITY CLASSIFICATION OF THIS PAGE (When Data Entered)

filaments around the inserted flagellum. After 5 minute incubation period, the parasites attached to the P388D did not show preferred orientation. At this time, numerous pseudopods and aggregated microfilaments of the P388D were seen around the invading parasites. When the relationship between the cytochalasin B-treated promastigotes and P388D were examined, no interaction of the promastigote flagella with P388D was observed at 2 minutes. After 5 minute incubation period, 50% of the attached parasites adhered to P388D without any particular orientation. When the interaction between the promastigotes and cytochalasin B-treated P388D were examined, the cytochalasin-treated cells showed fewer pseudopods than the untreated cells, and the number of parasites attached to them was reduced considerably after a 5 minute incubation period. This data demonstrated that the mode of entry by Leishmania promastigotes into macrophage-like P388D is dependent on the activation of the cells following the attachment of Leishmania promastigotes.

Studies on the structural alteration of erythrocyte membrane during malarial parasite invasion and during subsequent intraerythrocytic development were performed. Erythrocyte entry by malarial merozoites caused structural alteration of the erythrocyte membrane. Entry of the erythrocytes by the merozoites required the formation of a junction between the erythrocyte membrane and the apical end of the merozoite. Freeze-fracture showed that the junction consists of a narrow band of rhomboidally arrayed particles on the P face of the erythrocyte membrane and matching rhomboidally arrayed pits on the E face. IMP on the P face of the erythrocyte membrane disappear beyond this junction, resulting in the absence of IMP on the P face of the parasitophorous vacuole membrane which originated from the erythrocyte membrane. The sealing of the erythrocyte membrane is accomplished by fusion of the junction at the posterior end of the merozoite in the fashion of an iris diaphragm. After completion of the erythrocyte entry, the merozoite is surrounded by a parasitophorous membrane which is different in the molecular organization from the original erythrocyte membrane.

Two types of erythrocyte membrane modification were induced by the intraerythrocyte parasites. They include electron-dense protrusion called knobs and caveola-vesicle complexes on the erythrocyte membrane. Thin section electron microscopy showed many knobs on the erythrocytes infected with P. falciparum. Scanning electron microscopy demonstrated numerous cone-shaped knobs evenly distributed over the entire erythrocyte surface. Freeze-fracture and etching demonstrated that the knobs were protruded structures. The P face of the infected erythrocyte membrane showed evenly distributed IMP and no aggregation or depletion of IMP can be observed over the erythrocyte membrane covering the knobs. Unaltered IMP distribution on the knob portion of the erythrocyte membrane may correlate with the unaltered surface charge on the erythrocyte membrane covering the knobs.

In addition, we studied by electron microscopy the effects of monoclonals on epimastigotes and metacyclic stages of Trypanosoma cruzi. The metacyclic stages of T. cruzi were covered with a thick surface coat when they were incubated with monoclonal B 2/5. Adhesion between the surface coat of these parasites produced agglutination of these parasites. The agglutination caused by the monoclonal is specific to this stage. No agglutination of the parasites took place between the parasites when incubated with anti- P. knowlesi antibody. Incubation of the parasites with higher concentration of the monoclonals resulted almost immediately in a drastic reduction of parasite motility.

Summary

During this fiscal year, in collaboration with Col. Hendricks and his associates we studied the interactions between macrophage-like cells (P388D) and Leishmania braziliensis in vitro under various conditions by light and electron microscopy. When P388D and L. braziliensis were incubated together for two minutes, 90% of the promastigotes were attached to P388D by the tip of the flagella. The P388D did not form pseudopods or aggregated microfilaments around the inserted flagellum. After 5 minute incubation period, the parasites attached to the P388D did not show preferred orientation. At this time, numerous pseudopods and aggregated microfilaments of the P388D were seen around the invading parasites. When the relationship between the cytochalasin B-treated promastigotes and P388D were examined, no interaction of the promastigote flagella with P388D was observed at 2 minutes. After 5 minute incubation period, 50% of the attached parasites adhered to P388D without any particular orientation. When the interaction between the promastigotes and cytochalasin B-treated P388D were examined, the cytochalasin-treated cells showed fewer pseudopods than the untreated cells, and the number of parasites attached to them was reduced considerably after a 5 minute incubation period. This data demonstrated that the mode of entry by Leishmania promastigotes into macrophage-like P388D is dependent on the activation of the cells following the attachment of Leishmania promastigotes.

Studies on the structural alteration of erythrocyte membrane during malarial parasite invasion and during subsequent intraerythrocytic development were performed. Erythrocyte entry by malarial merozoites caused structural alteration of the erythrocyte membrane. Entry of the erythrocytes by the

merozoites required the formation of a junction between the erythrocyte membrane and the apical end of the merozoite. Freeze-fracture showed that the junction consists of a narrow band of rhomboidally arrayed particles on the P face of the erythrocyte membrane and matching rhomboidally arrayed pits on the E face. IMP on the P face of the erythrocyte membrane disappear beyond this junction, resulting in the absence of IMP on the P face of the parasitophorous vacuole membrane which originated from the erythrocyte membrane. The sealing of the erythrocyte membrane is accomplished by fusion of the junction at the posterior end of the merozoite in the fashion of an iris diaphragm. After completion of the erythrocyte entry, the merozoite is surrounded by a parasitophrous membrane which is different in the molecular organization from the original erythrocyte membrane.

Two types of erythrocyte membrane modification were induced by the intraerythrocyte parasites. They include electron-dense protrusion called knobs and caveola-vesicle complexes on the erythrocyte membrane. Thin section electron microscopy showed many knobs on the erythrocytes infected with P. falciparum. Scannning electron microscopy demonstrated numerous cone-shaped knobs evenly distributed over the entire erythrocyte surface. Freeze-fracture and etching demonstrated that the knobs were protruded structures. The P face of the infected erythrocyte membrane showed evenly distributed IMP and no aggregation or depletion of IMP can be observed over the erythrocyte membrane covering the knobs. Unaltered IMP distribution on the knob portion of the erythrocyte membrane may correlate with the unaltered surface charge on the erythrocyte membrane covering the knobs.

In additon, we studied by electron microscopy the effects of monoclonals on epimastigotes and metacyclic stages of Trypanosoma cruzi. The metacyclic

stages of T. cruzi were covered with a thick surface coat when they were incubated with monoclonal B 2/5. Adhesion between the surface coat of these parasites produced agglutination of these parasites. The agglutination caused by the monoclonal is specific to this stage. No agglutination of the parasites took place between the parasites when incubated with anti- P. knowlesi antibody. Incubation of the parasites with higher concentration of the monoclonals resulted almost immediately in a drastic reduction of parasite motility.

Foward

In conducting the research described in this report, the investigators adhered to the Guide for Laboratory Animal Facilities and Care, as promulgated by The Committee on The Guide for Laboratory Animal Resources, National Academy of Science - National Research Council.

Table of Contents

Detailed Report

a) Interactions Between Macrophage-Like Cells and *Leishmania braziliensis in vitro*.

b) Structural Alteration of Erythrocyte Membrane During Malarial Parasite Invasion and During Subsequent Intraerythrocytic Development.

c) Electron Microscopy of Knobs in *P. falciparum* Infected Erythrocytes.

d) Monoclonal Antibodies to *Trypanosoma cruzi* Inhibit Motility and Nucleic Acid Synthesis of Culture Forms.

AJP-81-348

Interactions Between Macrophage-Like Cells and Leishmania braziliensis In Vitro

Masamichi Aikawa, MD[1], Larry D. Hendricks, PhD[2],

Yoshihiro Ito, PhD[1], and Martin Jagusiak[2]

Institute of Pathology, Case Western Reserve University, Cleveland, Ohio 44106[1]

and

Division of Experimental Therapeutics, Walter Reed Army Institute of Research, Washington, D.C. 20012[2]

Running Title: Interactions Between Macrophages and Leishmania

Acknowledgements

This work was partially supported by the U.S. Army R & D Command Research Contract (C-9020). The authors wish to thank Maj. J. Berman for his advice on the manuscript.

Abstract

The interaction between macrophage-like cells (P388D murine tumor cells) and Leishmania braziliensis panamensis promastigotes was studied in vitro under various conditions by light and electron microscopy. When the macrophage-like cells and L. braziliensis were incubated together for 2 minutes, 90% of the promastigotes were attached to the macrophage-like cells by the tip of the flagella. The macrophage-like cells did not form pseudopods or aggregated microfilaments around the inserted flagellum. After a five minute incubation period, the parasites attached to the macrophage-like cells did not show preferred orientation. At this time, numerous pseudopods and aggregated microfilaments of the macrophage-like cells were seen around the invading parasites. When the relationship between the cytochalasin B-treated promastigotes and the macrophage-like cells were examined, no interaction of the promastigote flagella with macrophage-like cells was observed at 2 minutes. After a 5 minute incubation period, 50% of the attached parasites adhered to a macrophage-like cell without any particular orientation. When the interaction between the promastigotes and cytochalasin B-treated macrophage-like cells were examined, the cytochalasin B-treated cells showed fewer pseudopods than the untreated cells, and the number of parasites attached to them was reduced considerably after a 5 minute incubation period. This data demonstrated, for the first time, that the mode of entry by Leishmania promastigotes into macrophage-like cells is dependent on the activation of the macrophage-like cells following the attachment of Leishmania.

INTRODUCTION

Leishmania braziliensis is a causative protozoan parasite of cutaneous leishmaniasis and is found to be an intracellular, non-flagellated amastigote form within the reticuloendothelial cells of the mammalian host. When the amastigote form is taken up by sandflies, it develops into the promastigote form in the intestine of the insect. Mammalian infections are initiated by the insect vector, sandflies, which inoculate extracellular, flagellate promastigotes into the skin. Because the macrophages of mammalian hosts may be the cells which first interact with the promastigote, many investigators[1-6] have studied the interaction between these cells using both light and electron microscopy. However, there has not been a general agreement as to how the promastigote gains entry into the macrophage. Some experiments supported the active, flagellum-first entry by the parasite[7-10] and the others suggested non-oriented entry by macrophage phagocytosis[1-5,11].

In order to clarify whether or not the promastigotes' flagellum is involved in the interaction with the macrophages, we studied the interaction between the macrophage-like murine tumor cells and *L. braziliensis panamensis* promastigotes *in vitro* by light and electron microscopy, since the macrophage-like murine tumor cells react to *Leishmania* in a manner identical to that of normal macrophages[15]. Entry in the presence of cytochalasin B was studied to determine the importance of microfilament movements in the parasite and/or the macrophage[14]. The course of entry was also investigated to determine if significant parameters change with time.

MATERIALS AND METHODS

(1) Macrophage-Like Cells and Leishmania

The macrophage-like murine tumor cell line (P388D) was kindly provided by Dr. J.J. Marr of St. Louis University School of Medicine. Macrophage-like tumor cells were reported to phagocytize the amastigotes of L. donovani rapidly and proved to serve as a model host without the inherent limitations of the primary macrophage cultures[13]. Therefore, we used this cell line for our experiments. Cells were grown in suspension in a $25cm^2$ plastic tissue culture flask using Eagle's minimum essential medium (MEM) with spinner salts supplemented with 10% (v/v) heat-inactivated fetal bovine serum (FBS). The cultures were maintained at 37°C in a 5% (v/v), CO_2 atmosphere. Population density of 10^7 cells/ml were achieved in ≈ 10 days under these culture conditions.

In preparation for the infection experiments, the cells were taken from suspension cultures that were in a log phase, centrifuged at 800g for 20 min., resuspended in MEM in Hank's balanced salt solution (HBSS) with 10% FBS at a final density of 5×10^5 cells/ml. Aliquotes (2ml) of this suspension were placed in Leighton tubes containing 9 x 35mm coverslips and incubated for 24 hrs. at which time the medium was changed. There were approximately 350,000 macrophages per coverslip at this time. Leishmania braziliensis panamensis, WR 128, originally isolated from a U.S. soldier in Panama, was maintained as a stablaite in The Leishmania Section, Department of Parasitology, WRAIR, liquid nitrogen cryobank prior to use. The parasites proved to be infective against Mystromys albicaudatus and are being used as an excellent model of American cutaneous leishmaniasis in anti-leishmanial drug screen tests at WRAIR[15].

The stablaite was thawed quickly and the organisms were maintained in

Schneider's Drosophila Medium, Revised (GIBCO), plus 30%, v/v heat-inactivated FBS[13], until used. Promastigotes in log growth were added to each Leighton tube at a concentration of 4×10^7/ml and then incubated at 37°C. After incubation periods of 2, 5 and 60 minutes, the coverglasses were washed twice in HBSS to remove the free promastigotes, then fixed with 2.5% glutaraldehyde containing 4% sucrose and 0.1M cacodylate buffer (pH 7.4). The washing and fixation of the cells was conducted with the coverglasses still in their respective Leighton tubes. These experiments were repeated three times in order to ascertain the reproductivity of the experimental data.

(2) Cytochalasin B Experiments.

Promastigotes in MEM + 10% PBS were incubated at room temperature with a concentration of 10µg/ml of cytochalasin B to 0.1% dimethylsulfoxide (DMSO) (Promastigotes handled in the same manner but with only 0.1% DMSO added served as controls). A three-minute ambient temperature (24-26°C) incubation was followed by a brief warming to 37°C before cytochalasin B was removed by centrifugation washing (800g x 20 min.) in HBSS. The cytochalasin B-treated promastigotes were immediately added to the culture tubes containing untreated macrophage-like cells and incubated at 37°C. After 2 and 5 minutes, the samples were fixed. Alternately the macrophage-like cells were treated with cytochalasin B (10µg/ml) for 3 minutes, washed briefly in HBSS and exposed to untreated promastigotes in a similar manner. Samples for electron microscopy were fixed again at two and five minutes. This experiment was repeated three times.

(3) Electron Microscopy.

Samples fixed in 2.5% glutaraldehyde solution were washed in 0.1M cacody-

late buffer several times and then post-fixed in 1% osmium tetroxide for one hr. After dehydrating in an ascending concentration of alcohol, the samples were embedded in Spurr. The resulting blocks were cut with a Porter-Blum MT-2 ultramicrotome. Several thick sections (1μ thick) were obtained from each experiment, stained with 1% toluidene blue solution and were studied by light microscopy for quantitative analaysis of parasite-macrophage-like cell attachment. At least 200 macrophage-like cells were counted for the quantitative analysis of the attachment. Differences between the experiments were evaluated by the Student's "t" test.

Thin sections were placed on copper grids and stained with 1% uranyl acetate and lead citrate. The sections were examined with a JEOL 100CX electron microscope.

RESULTS

(1) Interaction between macrophage-like cells and promastigotes (both untreated).

The percentage of macrophage-like cells with attached promastigotes increased from 42.02 ± 3.9 at 2 minutes to 55.68 ± 4.2 at five minutes to 66.48 ± 2.8 at 60 minutes (Table 1). In three different sets of experiments, the average number of attached promastigotes per infected macrophage-like cell were 2.26 ± 0.32 at 2 minutes, 5.06 ± 0.45 at 5 minutes and 5.76 ± 0.82 at 60 minutes (Table 2).

When the 2 minute preparations were examined by light and electron microscopy, 90% of the attached promastigotes were attached to the macrophage-like cells by the tip of the flagellum (Figs. 1,3,4), while the remaining were attached to the macrophage-like cells without any particular orientation. After

a 5 minute incubation period, the attachment of promastigotes to the macrophages did not show preferred orientation (Fig. 2). While fifty percent of the promastigotes were attached to the macrophage-like cells with their flagellar tips (Fig. 5), the other 50% showed no particular orientation in relation to the macrophage-like cells. A similar observation was made between the promastigotes and the macrophage-like cells after a 60 minute incubation period. Even though the insertion of the flagellar tips into the macrophage-like cells was observed during the 2 minute incubation period, the macrophage-like cells did not form pseudopods or aggregated microfilaments around the flagellum (Fig. 4). However, pseudopods were formed around the inserting flagellum after both 5 and 60 minutes of incubation (Figs. 5 & 6). In these instances, aggregates of microfilaments in the cytoplasm of macrophage-like cells were observed adjacent to the inserted flagellum (Fig. 7). Several areas of close contact between the flagellar membrane and the invaginated plasma membrane of the macrophage-like cells were also observed (Fig. 7).

(2) <u>The interaction between cytochalasin B-treated promastigotes and untreated macrophage-like cells.</u>

The percentage of macrophage-like cells with attached cytochalasin B-treated promastigotes was 26.43 ± 1.72 after two minutes of incubation and 52.73 ± 3.96 after 5 minutes of incubation (Table 1). The average number of attached promastigotes per infected macrophage-like cell were 1.47 ± 0.12 at 2 minutes and 2.50 ± 0.31 at 5 minutes (Table 2).

At 2 minutes, no interaction of the promastigote flagella with the macrophage-like cells was observed. After a 5 minute incubation period, approximately 50% of the attached promastigotes adhered to the macrophage-like cells

without any particular orientation and the remainder were attached to the macrophage-like cell via their flagellum. There were pseudopod formations, aggregation of microfilaments and vesicles in the cytoplasm of the macrophage-like cells around the parasite attachment site (Fig. 8). The results of the interaction between the promastigotes treated with 0.1% DMSO and the macrophage-like cells were similar to those found between the untreated promastigotes and the macrophage-like cells.

(3) The interaction between promastigotes and cytochalasin B-treated macrophage-like cells.

The percentage of cytochalasin B-treated macrophage-like cells with attached promastigotes were 36.41 ± 1.22 at a 2 minute incubation period and 39.42 ± 1.07 at a 5 minute incubation (Table 1). The average number of attached promastigotes per infected macrophage-like cell were 2.74 ± 0.30 at a 2 minute incubation period and 2.36 ± 0.39 at a 5 minute incubation period (Table 2).

Cytochalasin B-treated macrophage-like cells showed fewer pseudopods during the interaction with promastigotes than with untreated macrophage-like cells. After a 2 minute incubation period, about 80% of the promastigotes attached to the macrophage-like cells showed the insertion of the flagellum into the cytoplasm. The remainder of the promastigotes were attached to the membrane of macrophage-like cells without any particular orientation. Few pseudopods were present around the parasites. After a 5 minute incubation period, about 50% of the attached promastigotes showed their flagellum inserting into the cytoplasm of the macrophage-like cells (Fig. 9). Again, the pseudopod formation was not prominent. Ninety percent of the promastigotes inserted their flagellum into the cytoplasm of DMSO-treated macrophage-like cells at 2 minutes incubation.

DISCUSSION

Interactions between the macrophages and leishmanial promastigotes have been studied extensively to elucidate the mechanism of macrophage entry by the promastigotes[1-12]. However, whether the macrophages engulf the leishmanial promastigotes by phagocytosis or the parasite actively penetrates the cell has been controversial. Pulvertalf and Hoyle[10] demonstrated that the promastigotes of L. donovani enter the hamster macrophages by inserting their flagellar tip first, indicating that the parasites actively enter the macrophages. A similar observation was made by Miller and Twohy[9]. Lewis[7] found that L. mexicana promastigotes could infect the sarcoma cells in spite of the presence of cytochalasin B and suggested that the promastigote plays an active role in the host cell infection. Conversely, other model systems have demonstrated abundant macrophage pseudopods around the promastigotes, no preferable orientation of the parasite during entry and inhibition of the parasite entry by cytochalasin B, supporting the importance of the macrophage phagocytosis mechanisms. For example, Akiyama and Haight[2] reported that most of the promastigotes of L. donovani were first engulfed at the posterior end and L. mexicana promastigote entry was inhibited by cytochalasin B. Chang[4], using scanning and transmission electron microscopy, reported that the promastigotes of L. donovani depend on phagocytic activity of macrophages to gain intracellular entrance although he suggested that the parasite-specific activities and/or properties might also play a role in the parasite entry.

In the present work, the initial (two minute) interaction of promastigotes with macrophage-like cells was almost completely via the flagellum. After 5 minutes, the promastigotes were attached to the macrophage-like cells without any

particular orientation and were surrounded by numerous pseudopodia which contained aggregate microfilaments, contractile structures associated with phagocytosis[17-19]. These observations suggest that the promastigotes of L. braziliensis actively enter into the macrophage-like cells with the flagellum end first during the first 2 minute interaction period. After 5 minutes, the macrophage-like cells start to exhibit phagocytic activity and the phagocytic processes become important for parasite entry. This postulation is also supported by statistical data which shows an increase in the percentage of macrophage-like cells which had promastigotes attached as the incubation period increases. Macrophages are known to be activated within 10 minutes after stimulation[17]. It is likely that the macrophage-like cells become activated by the parasites in 5 minutes, and the phagocytic activity of the macrophage-like cells as well as active attachment processes by the promastigotes contribute to the entry of the parasites into the macrophage-like cells at this time.

Our experiments with cytochalasin B-treated promastigotes or macrophage-like cells also support these conclusions. The fact that the number of cytochalasin B-treated macrophage-like cells with attached promastigotes did not increase in spite of the longer incubation periods, indicates that inhibition of phagocytic uptake of Leishmania by cells during the 5 minute incubation period. Reduction in the attachment of cytochalasin B-treated promastigotes to untreated macrophage-like cells at 2 minutes when compared to that of untreated parasites, again suggests that promastigote-specific activities are important in parasite entry at 2 minutes. The lack of flagellum attachment in such experiments suggests that the promastigote microfilament movement is important for the parasite flagellum attachment and entry into the macrophage-like cells during the 2 minute time frame. Although Ardehali et al.[1] concluded that

Leishmania enter the macrophages by phagocytosis based on their experiment using cytochalasin B, their data is derived from observations of 8 hour incubation of parasites and macrophages. Their data is similar to ours at 60 minute incubation time, when phagocyic activity accounts for the entry of the parasites.

In conclusion, our report demonstrated that promastigotes of L. braziliensis actively enter into the macrophage-like cells with their flagellar ends first during the first 2 minute incubation period. After this initial period, macrophage-like cells are activated by the parasites and start to exhibit phagocytic activity and the phagocytic processes become important to parasite entry. Therefore, the mode of entry by Leishmania promastigotes into macrophages is dependent on the activation of macrophages following the attachment of the parasites.

REFERENCES

1. Andehall SM, Khoubyar K, Rezai HR: Studies on the effect of antiphagocytic agent cytochalasin B on Leishamania-macrophage interaction. Acta Tropica 1979, 36:15-21.

2. Akiyama HJ, Haight RD: Interaction of Leishmania donovani and hamster peritoneal macrophages. Am J Trop Med Hyg 1971, 20:539-545.

3. Alexander J: Effect of antiphagocytic agent cytochalasin B on macrophage invasion by Leishmania mexicana promastigotes and Trypanosoma cruzi epimastigotes. J Protozool 1975, 22:237-240.

4. Chang KP: Leishmania donovani: Promastigote-macrophage surface interactions in vitro. Expt Parasitol 1979, 48:175-189.

5. Chang KP: Leishmania donovani-hamster macrophage binding mediated by their surface glycoproteins/antigens: Characterization in vitro by a radioisotopic assay. Mol Biochem Parasitol 1981, 4:67-76.

6. Chang KP, Dwyer DM: Leishmania donovani: Hamster macrophage interactions in vitro: Cell entry, intracellular survival and multiplication of amastigotes. J Exp Med 1978, 147:515-530.

7. Lewis DH: Infection of tissue culture cells of low phagocytic ability by Leishmania mexicana mexicana. Ann Trop Med Parasitol 1974, 68:327-336.

8. Merino F, Ajiam E, Hernandez A, Dawidowicz K, Merino EJ: In vitro infection of murine macrophage by Leishmania braziliensis: Mechanisms of penetration. Int Archs Allergy Appl Immunol 1977, 55:487-495.

REFERENCES (cont'd)

9. Miller HC, Twohy DW: Infection of macrophages in culture by leptomonads of Leishmania donovani. J Protozool 1967, 14:781-189.

10. Pulvertaft RJV, Hogle GF: Stages in the life cycle of Leishmania donovani. Trans Roy Soc Trop Med & Hyg 1960, 54:191-196.

11. Pearson R, Romito R, Symes P, Harcus J: Interaction of Leishmania donovani promastigotes with human monocyte-derived macrophages: Parasite entry, intracellular survival and multiplication. Infection & Immunity 1981, 32:1249-1253.

12. Zenian A, Rowles P, Gingell D: Scanning electron microscopic study of the uptake of Leishmania parasites by macrophages. J Cell Sci 1979, 39:187-199.

13. Berens RL, Marr JJ: Growth of Leishmania donovani amastigotes in a continuous macrophage-like cell culture. J Protozool 1979, 26:453-456.

14. Miller LH, Aikawa M, Johnson J, Shiroishi T: Interaction between cytochalasin B-treated malarial parasites and erythrocytes: Attachment and junction formation. J Exp Med 1979, 149:172-184.

15. McKinney LA, Hendricks LD: Experimental infection of Mystromys albicaudatus with Leishmania braziliensis: Pathology. Am J Trop Med Hyg 1980, 29:753-760.

16. Hendricks LD, Wood DE, Hajduk ME: Haemoflagellates: Commercially available liquid media for rapid cultivation. J Parasitol 1978, 76:309-316.

REFERENCES (cont'd)

17. Cohn ZA: The activation of mononuclear phagocytes: Fact, fancy and future. J Immunol 1978, 121:813-816.

18. Mazur MT, Williamson JR: Macophage deformability and phagocytosis. J Cell Biol 1977, 75:185-199.

19. Reaven EP, Axline SG: subplasmalemmal microfilaments and microtubules in resting and phagocytizing cultivated macrophages. J Cell Biol 1973, 59:12-27.

Figure Legends

Fig. 1 Light micrograph showing the interaction between promastigotes and macrophage-like cells after a 2 minute incubation period. Most of the parasites attach to the latter with their flagellum (arrow). X 1,000.

Fig. 2 Light micrograph showing the interaction between the promastigotes and macrophage-like cells after a 5 minute incubation period. Many parasites attach to the macrophage-like cells without any particular orientation. X 1,000.

Fig. 3 Electron micrograph showing insertion of the flagella (arrow) of many promastigotes into a macrophage-like cell after a 2 minute incubation period. X 10,000.

Fig. 4 High magnification electron micrograph showing insertion of the flagellum (arrow) of a promastigote into a macrophage-like cell after a 2 minute incubation period. No pseudopod formation is seen at the site of the flagellum insertion. X 28,000.

Fig. 5 Electron micrograph showing insertion of the promastigote's flagellum (arrow) deep into a macrophage-like cell after a 5 minute incubation period. A few pseudopods (P) and vesicles (V) are seen around the inserted flagellum. X 7,000.

Fig. 6 Electron micrograph showing the interaction between promastigotes and macrophage-like cells after a 60 minute incubation period. Many parasites are attached to the macrophage-like cells without any particular orientation. Note pseudopodia (arrow) of macrophage-

Figure Legends (cont'd)

Fig. 6 like cells extending around the parasites. X 4,500.

Fig. 7 High magnification electron micrograph showing aggregations of microfilaments (arrow) and vesicles around the inserted flagellum of a L. brasiliense promastigote after a 5 minute incubation period. Note several contacts (C) between the flagellar and macrophage-like cell membranes. X 60,000.

Fig. 8 Electron micrograph showing a cytochalasin-treated promastigote entering a macrophage after a 5 minute incubation period. Pseudopod formation (arrow) is seen at the site of the parasite entry. X 27,000.

Fig. 9 Electron micrograph showing insertion of the flagellum of the parasite (L) into a cytochalasin-treated macrophage-like cell after a 5 minute incubation period. There are only a few, short pseudopods (arrow) around the inserted flagellum. X 19,000.

Table 1

Percentage of Macrophage-Like Cells (P388D) With Attached Promastigotes

Incubation Time	Both Untreated[a]	Cytochalasin-Treated Promastigotes[b]	Cytochalasin-Treated P388D Cells[c]
2 min.	42.02 ± 3.9	26.43 ± 1.72	36.41 ± 1.22
5 min.	55.68 ± 4.2	52.73 ± 3.96	39.42 ± 1.07
60 min.	66.48 ± 2.8		

a: There is significant difference ($P<0.05$) when compared with 2 minute, 5 minute and 60 minute incubation times and with 2 minute and 60 minute incubations.

b: Significant difference ($P<0.05$) exists between 2 minute and 5 minute incubation times.

c: No significant difference between 2 and 5 minute incubation times.

Table 2

Mean Number of Attached Promastigotes Per Each Infected P388D Cell

Incubation Time	Both Untreated[a]	Cytochalasin-Treated Promastigotes[b]	Cytochalasin-Treated P388D Cells[c]
2 min.	2.26 ± 0.32	1.47 ± 0.12	2.74 ± 0.30
5 min.	5.06 ± 0.45	2.50 ± 0.31	2.36 ± 0.39
60 min.	5.76 ± 0.82	not performed	not performed

a: There is a significant difference ($P<0.05$) in the values obtained between the 2 minute and 5 minute times and between the 2 minute and 60 minute incubation times. No significant change is found between the 5 minute and 60 minute incubations.

b: Significant difference ($P<0.05$) exists between 2 minute and 5 minute incubations.

c: There is no significant difference between 2 minute and 5 minute incubations.


1
2


P
5

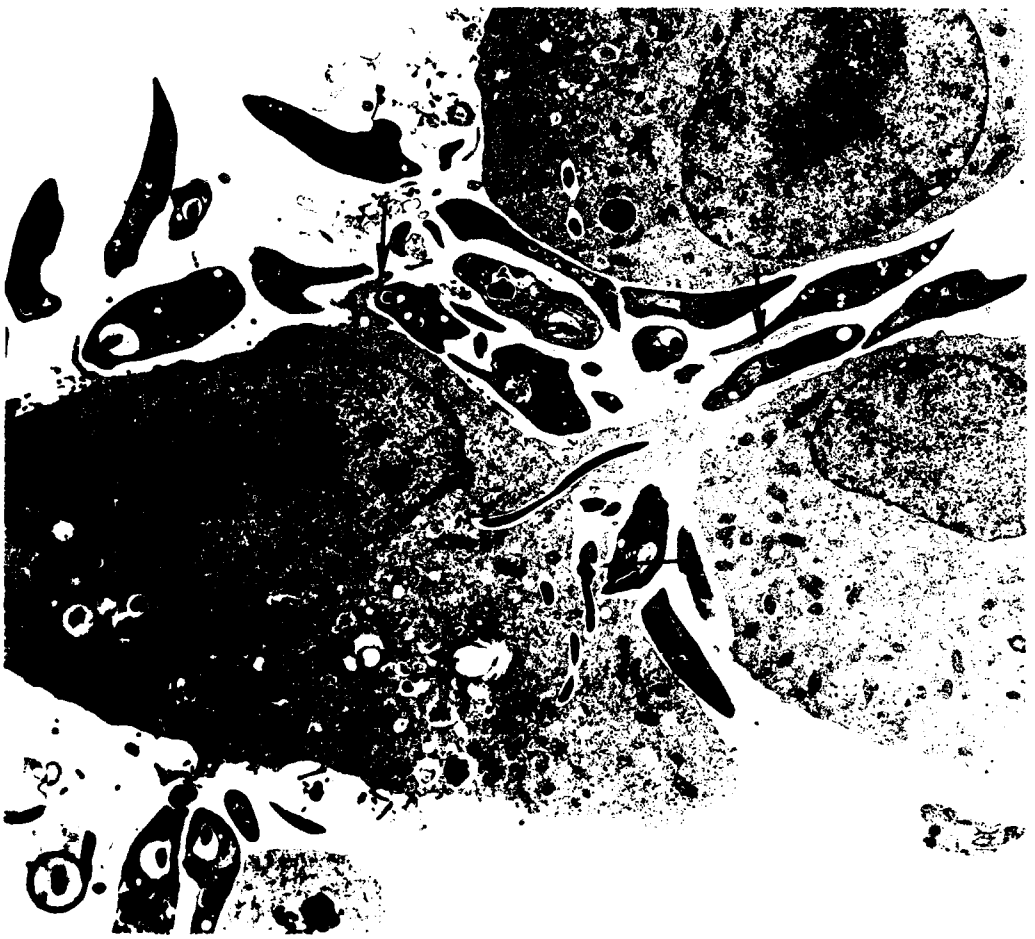

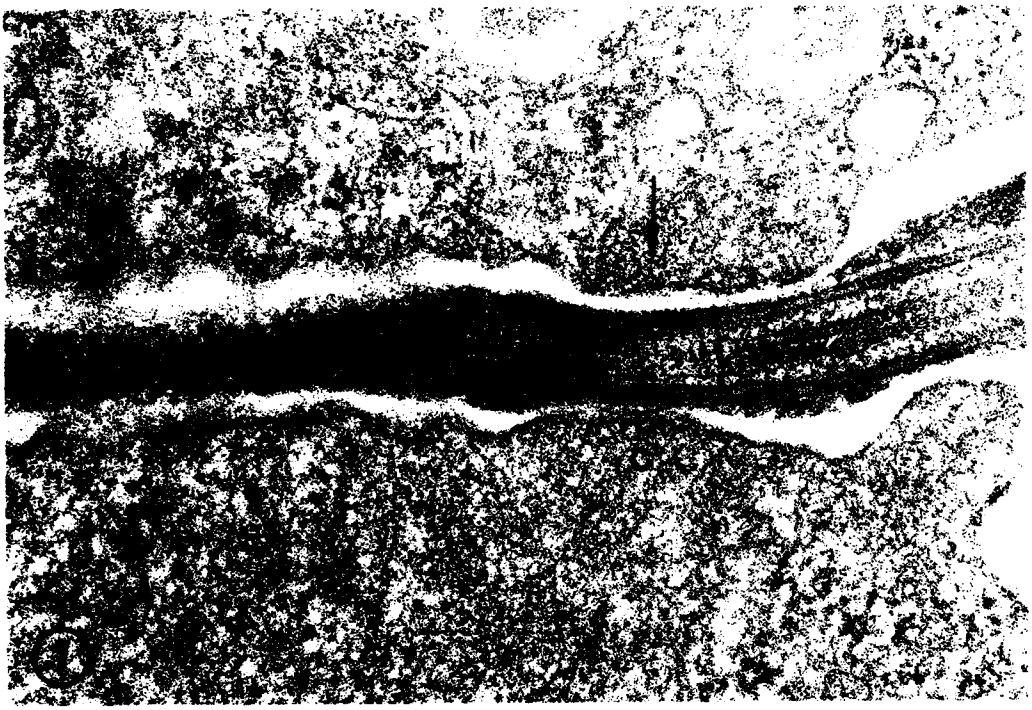

(9)

Structural Alteration of Erythrocyte Membrane During Malarial Parasite Invasion and During Subsequent Intraerythrocytic Development

Masamichi Aikawa[1] and Louis H. Miller[2]

[1] Institute of Pathology, Case Western Reserve University, Cleveland, Ohio, 44106 U.S.A.

and

[2] Laboratory of Parasitic Diseases, National Institute of Allergy and Infectious Diseases, Bethesda, Maryland, 20205, U.S.A.

Acknowledgements

This work was supported in part by Research Grants (AI-10645 and AI-13366) from the U.S. Public Health Service, by the U. S. Army R & D Command (DAMD 17-79-C-9029) and the World Health Organization (T16/181/M2/52).

Abstract

Erythrocyte entry by malarial merozoites causes structural alteration of the erythrocyte membrane. First, entry of the erythrocytes by the merozoites requires the formation of a junction between the erythrocyte membrane and the apical end of the merozoite. Secondly, migration of the junction parallel to the long axis of the merozoite brings the merozoite into an invagination of the erythrocyte membrane. Freeze-fracture shows that the junction consists of a narrow band of rhomboidally arrayed particles on the P face of the erythrocyte membrane and matching rhomboidally arrayed pits on the E face. IMP on the P face of the erythrocyte membrane disappear beyond this junction, resulting in the absence of IMP on the P face of the parasitophorous vacuole membrane which originated from the erythrocyte membrane. The sealing of the erythrocyte membrane is accomplished by fusion of the junction at the posterior end of the merozoite in the fashion of an iris diaphragm. After completion of the erythrocyte entry, the merozoite is surrounded by a parasitophorous vacuole membrane which is different in the molecular organization from the original erythrocyte membrane. In addition, two types of erythrocyte membrane modification are induced by the intraerythrocyte parasites. They include electron-dense protrusions called knobs and caveola-vesicle complexes along the erythrocyte membrane.

Introduction

Invasion of erythrocytes by malarial merozoites is the initial step for the development of the erythrocytic stages of malarial parasites. The information that has accumulated in recent years demonstrates that the merozoites enter the erythrocytes by a definite sequence: 1) initial recognition and attachment of the merozoite to the erythrocyte membrane, 2) junction formation between the apical end of the merozoite and the erythrocyte, 3) creation of a vacuole membrane which is continuous with the erythrocyte membrane, 4) entry of the parasite into the vacuole by a moving junction around the merozoite, and 5) sealing of the erythrocyte and vacuole membranes after completion of the merozoite invasion (Aikawa et al. 1978, Bannister et al. 1975, Dvorak et al. 1975).

In this chapter, we will focus on the events defined by ultrastructural studies which explain how the merozoite of limited mobility can enter an erythrocyte, and how the structure of the erythrocyte membrane alters during these processes. In addition, we will discuss the alterations in the erythrocyte membranes induced by the intraerythrocytic parasites.

1) Recognition and Attachment Between the Merozoite and Erythrocyte.

Since understanding the structure of the malarial merozoite is important in analyzing the interaction between the erythrocytes and merozoites, a brief description of the merozoite is given. The merozoite is surrounded by a pellicular complex of two membranes and a row of subpellicular microtubules. The apical end is a truncated cone-shaped structure demarcated by polar rings. Electron-dense rhoptries and micronemes are seen in the apical end; ductules from the rhoptries extend to the tips of the apical end.

The initial factor underlying attachment between the merozoites and erythrocytes may be the difference in the surface charge of the erythrocyte and merozoite. Cytochemical studies, using positively-charged colloidal ions, have indicated that the merozoite membrane is less negatively charged in relation to the erythrocyte membrane (Seed et al. 1974). Initially, merozoites can attach to the erythrocytes in any orientation, but for a successful entry they reorient themselves so that the apical end of the merozoite becomes attached to the erythrocyte membrane (Dvorak et al. 1975). There are several reports that indicate the presence of receptors on the erythrocyte membrane for the merozoites. These include the Duffy blood group antigens for P. knowlesi and P. vivax (Miller et al. 1975) and glycophorin for P. falciparum (Miller et al. 1977, Perkins 1981).

Under normal conditions, the erythrocyte membrane becomes slightly raised initially at the interaction point when the apical end of the merozoite contacts the erythrocyte membrane, but eventually a depression is created in the erythrocyte membrane (Fig. 1). The erythrocyte membrane to which the parasite is attached becomes thickened measuring about 15nm in thickness (Aikawa et al. 1978). This thickened membrane forms a junction with the parasite membrane in the area of close appositon between the merozoite and erythrocyte. The junctional gap between the erythrocyte membrane and merozoite membrane is about 10nm; fine fibrils extend between these two parallel membranes.

Human erythrocytes lacking the Duffy blood group antigens are resistant to invasion by the merozoites of P. knowlesi (Miller et al. 1975). Electron microscopy showed that no junction is formed between a Duffy negative erythrocyte and P. knowlesi merozoites (Miller et al. 1979). The apical end of

the merozoite is oriented toward the erythrocyte, but instead of a junction, the erythrocyte is about 120nm away from the merozoite and they are connected by thin filaments (Fig. 2). Such filamentous attachments between the merozoites and erythrocytes are not observed in the experiments with normal rhesus or human Duffy positive erythrocytes. On the other hand, trypsinization of the Duffy negative human erythrocytes permits a junction formation with the merozoites and invasion (Fig. 3). The absence of a junction formation with Duffy negative human erythrocytes may indicate that the Duffy associated antigen acts as a high affinity receptor for the junction formation (Miller et al. 1979). Recently, ovalocytic erythrocytes were reported to be resistant to P. falciparum invasion (Kidson et al. 1981). This resistance may relate to an alteration of the erythrocyte cytoskeleton, preventing redistribution of IMP for a junction formation (Wilson 1982).

2) Erythrocyte Entry

Following attachment of the merozoite to the erythrocyte membrane, some products from the rhoptries and micronemes participate in the invagination of the erythrocyte membrane. Throughout the invasion, the apical end remains in contact with the vacuole membrane through an electron-dense band which is continuous with the common duct of the rhoptries (Aikawa et al. 1978)(Fig. 4). Lower electron-density in the ductule during invasion suggests that rhoptry contents are released into the vacuolar membrane through this band. It is indicated that a histidine-rich protein may be located in the rhoptries (Kilejian 1974).

As the invasion progresses, the depression of the erythrocyte membrane which was created by the apical end of the merozoite deepens and conforms to the shape of the merozoite (Aikawa et al. 1978, Bannister et al. 1975) (Fig. 4).

The junction is no longer observed at the initial attachment point, but now appears at the orifice of the merozoite-induced invagination of the erythrocyte membrane (Fig. 4). As the merozoite invasion progresses, the junction, which is in the form of a circumferential zone of attachment between the erythrocyte and merozoite, moves along the confronted membranes to maintain its position at the orifice of the parasitophorous vacuole (Aikawa et al. 1978).

Freeze-fracture shows a narrow circumferential band of rhomboidally arrayed intramembrane particles (IMP) on the P face of the erythrocyte membrane at the orifice of the erythrocyte invagination (Fig. 5) and matching rhomboidally arrayed pits on the E face (Aikawa et al. 1981) (Fig. 6). The band corresponds to the junction between the erythrocyte and merozoite membranes observed in thin sections. This finding indicates that the IMP on the erythrocyte rearrange themselves at the site of Plasmodium entry for local membrane specialization (Satir 1980). Studies on membrane-membrane fusions have demonstrated that IMP are displaced laterally into adjacent membrane regions before the fusion process and that fusion occurs between protein-depleted lipid bilayers (Loyter and Lalazar 1980). In contrast to this lateral displacement of IMP, reorganization of IMP occurs at the site of the erythrocyte-merozoite interaction. Apparently, this difference arises because the interaction between the erythrocyte and parasite membranes at the junction site is a transient phenomenon and is not a fusion process.

The IMP on the P face of the erythrocyte membrane disappear beyond this junction (Fig. 5). Therefore, the P face of the parasitophorous vacuole membrane which originated from the erythrocyte membrane is almost devoid of IMP (Aikawa et al. 1981, McLaren et al. 1979). On the other hand, a small difference in the number of IMP was noted between the E face of the erythrocyte

membrane and the E face of the parasitophorous vacuole membrane (Aikawa et al. 1981) (Table 1). A small dimple measuring about 50nm in diameter is present on the P face of the parasite membrane at the tip of the apical end. This may correspond to the opening of the rhoptry duct present at the apical end of the merozoite (Aikawa et al. 1981). The contents of rhoptries have been suggested to be involved in the formation for the relatively protein-free vacuole membrane.

Based on these findings, one can conclude that the movement of the junction during invasion is an important component of the mechanisms by which the merozoite enters the erythroctye. This junctional movement may be related to the lateral displacement of the junction by the membrane flow on the merozoite. On the other hand, when the erythrocytes and cytochalsin B-treated merozoites are incubated together, the merozoite attaches to the erythrocyte membrane and a junction is formed between the two, but the invasion process does not advance further and no movement of the junction occurs (Miller et al. 1979). Although there is no entry of the parasite, the erythrocyte membrane still invaginates (Aikawa et al. 1981, Miller et al. 1979). Freeze-fracture showed that the P face of the invaginated erythrocyte membrane is also almost devoid of IMP. This suggests that the attachment process in and of itself is sufficient to create a relatively IMP-free bilayer of the parasitophorous vacuole.

3) Sealing of the Erythrocyte Membrane After Completion of the Merozoite Entry

When the merozoite entry is completed, the junction fuses at the posterior end of the merozoite, closing the orifice of the invagination in the fashion of an iris diaphragm (Aikawa et al. 1978) (Fig. 7). The merozoite membrane still remains in close apposition to the thickened erythrocyte membrane at the

point of the final closure (Fig. 8). These observations demonstrate that the junction plays an important role in sealing of the erythrocyte membrane after completion of the merozoite invasion.

After completion of the erythrocyte entry, the merozoite is surrounded by a membrane of the parasitophorous vacuole that originated from the erythrocyte membrane, but the vacuole membrane is different in the molecular organization from the original erythrocyte membrane.

4) Alteration of the Erythroctye Membrane During Intraerythrocytic Parasite Development.

Intraerythrocytic parasites not only influence the parasitophorous vacuole membrane but also the erythrocyte membrane itself. Two types of erythrocyte membrane modification can be seen in the erythrocytes infected with certain species of malarial parasites: (1) electron-dense protrusions called knobs (Aikawa et al. 1972, Luse and Miller 1971), and (2) caveola-vesicle complexes along the erythrocyte membrane (Aikawa et al. 1975).

The erythrocytes infected with small trophozoites show few knobs, but they increase in number as the parasite grows within the erythrocyte (Figs. 9 and 10). The erythrocyte membrane covering the knobs is immunologically different from the rest of the erythrocyte membrane (Kilejian et al. 1977, Langreth and Reese 1979). These knobs form focal junctions with the endothelial cell membranes (Fig. 11) or with the knobs of other erythrocytes, resulting in the sequestration of those infected erythrocytes along the vascular endothelium. To facilitate studies of the mechanism of attachment of parasitized erythrocytes to the endothelium, Udeinya et al. (1981) demonstrated that the knobs on P. falciparum-infected erythrocyte membranes are the points of attachment to cultured

human endothelial cells. The knobs concentrate in the area of the erythrocyte membrane in apposition with the endothelial cells and an aggregation of microfilaments in the endothelial cells is seen at the site of knob-erythrocyte attachment (Fig. 11). On the other hand, the knobs found on the membrane of the erythrocytes infected with P. malariae are morphologically identical to those found on the membrane of P. falciparum-infected erythrocytes, yet, these infected cells do not bind to the endothelial cells (Udeinya et al. 1981). Therefore, it is conceivable that the knobs of P. falciparum contain some components which are required for attachment, but are not present on the knobs of P. malariae.

Freeze-fracture and etch have demonstrated that the P face of the membrane of P. falciparum-infected erythrocytes covering the knobs shows evenly distributed IMP and no aggregation or depletion of IMP can be observed (Fig. 10). The E face showed many indentations which correspond to the knobs. However, no alteration of IMP distribution can be found over the knob regions (Aikawa et al. 1982). It is possible that IMP may change their distribution pattern at the time of focal junction formation with the endothelial cells, since it is known that IMP change their distribution at the site of junction formation (Staehelin 1974). Unaltered IMP distribution on the knob portion of the erythrocyte membrane may correlate with the unaltered charge on the erythrocyte membrane covering the knobs induced by P. coatneyi infection (Miller et al. 1972).

Caveola-vesicle complexes seen along the erythrocyte plasma membrane correspond to Schüffner's dots seen in the erythrocytes infected by vivax-and ovale-type parasites during light microscopy. They consist of caveolae surrounded by small vesicles in an alveolar fashion (Aikawa et al. 1975) (Fig. 12). Immuno-electron microscopy demonstrated the presence of malarial antigens within them. However, it is not clear how the malarial antigens move from the parasite to the

caveola-vesicle complexes. In addition, the infected erythrocyte cytoplasm shows narrow clefts which correspond to Maurer's clefts seen by light microscopy. The nature of the clefts is still unknown, but they probably originate from the parasitophorous vacuole membrane. Transmission electron microscopy showed extension of the cleft into the parsitophorous vacuole (Aikawa et al. 1975, Rudzinska and Trager 1968). The functional significance of caveola-vesicle complexes and clefts is still not clear and must await future investigation.

References

Aikawa M, Rabbege J, Udeinya I, Miller LH 1982 Electron microscopy of knobs in P. falciparum-infected erythrocytes. J Parasitol (In Press).

Aikawa M, Miller LH, Rabbege JR, Epstein N 1981 Freeze-fracture study on the erythrocyte membrane during malarial parasite invasion. J Cell Biol 91:55-62.

Aikawa M, Miller LH, Johnson J, Rabbege J 1978 Erythrocyte entry by malarial parasites: A moving junction between erythrocyte and parasite. J Cell Biol 77:72-82.

Aikawa M, Miller LH, Rabbege J 1975 Caveola-vesicle complexes: The plasmalemma of erythrocytes infected by Plasmodium vivax and Plasmodium cynomolgi. Am J Path 79:285-300.

Aikawa M, Rabbege J, Wellde BT 1972 Junctional apparatus in erythrocytes infected with malarial parasites. Z Zellfrosch 124:72-75.

Bannister LH, Butcher GA, Dennis ED, Mitchell GH 1975 Structure and invasive behavior of Plasmodium knowlesi merozoites in vitro. Parasitol 71:483-491.

Dvorak JA, Miller LH, Whitehouse WC, Shiroishi T 1975 Invasion of erythrocytes by malaria merozoites. Science 187:748-750.

Kidson C, Lamont G, Saul A, Nurse GT 1981 Ovalocytic erythrocytes from Melanesians are resistant to invasion by malaria parasites in culture. Proc Nat Acad Sci USA 78:5829-5832.

Kilejian A, Abati A, Trager W 1977 Plasmodium falciparum and Plasmodium coatneyi: Immunogenicity of "Knob-like protrusions" on infected erythrocyte membrane. Exp Parasitol 42:157-164.

Kilejian, A 1974 A unique histidine-rich polypeptide from the malaria parasite, Plasmodium lophurae. J Bio Chem 249:4650-4655.

Langreth SG, Reese RT 1979 Antigenicity of infected-erythrocyte and merozoite surface in Falciparum malaria. J Exp Med 150:1241-1245.

Loyter A, Lalazar A 1980 Induction of membrane fusion in human erythrocyte ghosts: Involvement of spectrin in the fusion process. In: Gilula NB (eds) Membrane-membrane interaction. Raven Press, New York, p 11-26.

Luse SA, Miller LH 1971 Plasmodium falciparum malaria: Ultrastructure of parasitized erythrocytes in cardiac vessels. Am J Trop Med Hyg 20:655-660.

McLaren DJ, Bannister LH, Trigg PI, Butcher GA 1979 Freeze-fracture studies on the interaction between the malaria parasite and the host erythrocyte in Plasmodium knowlesi infections. Parasitol 79:125-139.

Miller LH, Aikawa M, Johnson J, Shiroishi T 1979 Interaction between cytochalasin B-treated malarial parasites and red cells: Attachment and junction formation. J Exp Med 149:172-184.

Miller LH, Mason SJ, Dvorak M, McGinniss H, Rothman IK 1975 Erythrocyte receptors for (Plasmodium knowlesi) malaria: Duffy blood group determinants. Science 189:561-562.

Miller LH, Cooper GW, Chien S, Freemount HN 1972 Surface charge on Plasmodium knowlesi and P. coatneyi-infected red cells of Macaca mulatta. Exp Parasitol 32:86-95.

Perkins M 1981 Inhibitory effects of erythrocyte membrane proteins on the in vitro invasion of the human malarial parasite (Plasmodium falciparum) into its host cell. J Cell Biol 90:563-567.

Rudzinska M, Trager W 1968 The fine structure of trophozoites and gametocytes in Plasmodium coatneyi. J Protozool 15:73-88.

Satir BH 1980 The role of local design in membrane. In: Gilula NB (eds) Membrane-membrane interactions. Raven Press, New York, p 45-58.

Seed TM, Aikawa M, Sterling C, Rabbege JR 1974 Surface properties of extracellular malaria parasites: Morphological and cytochemical study. Infect Immun 9:750-761.

Staehelin LA 1974 Structure and function of intercellular junctions. Inter Rev Cytol 39:191-283.

Udeinya IJ, Schmidt JA, Aikawa M, Miller LH, Green I 1981 Falciparum malaria-infected erythrocytes specifically bind to cultured human endothelial cells. Science 213:555-557.

Wilson RJ 1982 How the malarial parasite enters the red blood cell. Nature 295:368-369.

Figure Legends

Fig. 1 Electron micrograph of a merozoite creating a depression in the erythrocyte membrane. The membrane becomes thickened at the attachment site (arrow).

Fig. 2 Plasmodium knowlesi merozoite is connected with a Duffy negative erythrocyte by fine filaments (arrow).

Fig. 3 A merozoite is attached to a trypsin-treated Duffy negative erythrocyte by forming a junction (arrow). Note the thickened erythrocyte membrane at the site of attachment (From: Miller et al. 1979 J Exp Med 149:1172).

Fig. 4 An advanced stage of erythrocyte (E) entry by a merozoite. A junction (J) now appears at the orifice of the merozoite-induced invagination of erythrocyte membrane. A narrow band (arrow) connects the apical end and the erythrocyte membrane. Inset: High magnification micrograph of the junction. (From: Aikawa, M et al. 1978 J Cell Biol 77:72).

Fig. 5 Freeze-fracture electron micrograph of erythrocyte entry by a merozoite. The P face (Pe) of the erythrocyte membrane at the neck of the invagination is covered with IMP, but they disappear beyond the point where the neck of the invagination abruptly expands to form a parasitophorous vacuole (Pv). Inset: A narrow band of rhomboidally arrayed IMP (arrow) can be seen on the P face of the erythrocyte membrane at the orifice of the erythrocyte invagination. (From: Aikawa, M et al. 1981 J Cell Biol 91:55).

Figure Legends (cont'd)

Fig. 6 Freeze-fracture electron micrograph of erythrocyte entry by a merozoite. The E face of the erythrocyte membrane at the neck of the invagination consists of a narrow circumferential band of rhomboidally arrayed pits (arrow). Ev is the E face of the vacuole membrane. Inset: High magnification micrograph showing a narrow band of rhomboidally arrayed pits. (From: Aikawa, M et al. 1981 J Cell Biol 91:55).

Fig. 7 Erythrocyte entry by a merozoite (M) is almost completed and a small orifice (arrow) is present at the posterior end of the merozoite. The junction (J) is now moved to the posterior end of the merozoite. (From: Aikawa, M et al. 1978 J Cell Biol 77:72).

Fig. 8 Erythrocyte entry by a merozoite is completed and the parasite is within a parasitophorous vacuole. However, the posterior end of the merozoite is still attached (arrow) to the thickened erythrocyte membrane. (From: Aikawa, M et al. 1978 J Cell Biol 77:72).

Fig. 9 Scanning electron micrograph showing numerous knobs (arrow) on the surface of the infected erythrocyte.

Fig. 10 Freeze-fracture electron micrograph showing knobs (arrow) on the surface of the infected erythrocyte. The distribution of IMP is not altered by the presence of these knobs.

Fig. 11 Knobs on the surface of the infected erythrocyte form focal junctions (arrow) with the endothelial cell membrane (En). Inset: High power micrograph showing aggregation of microfilaments in the endothelial cells at the site of knob-erythrocyte attachment.

Figure Legends (cont'd)

Fig. 12 Erythrocyte infected with P. vivax showing caveola-vesicle complexes (arrow) and clefts (C). Inset: High magnification micrograph showing a caveola-vesicle complex.

TABLE 1

Mean IMP Densities/μm^2 on the Erythrocyte and Vacuole Membranes

	P Face	E Face
Erythrocyte Membrane	2109 ± 431	389 ± 100
Vacuole Membrane	564 ± 148	334 ± 65

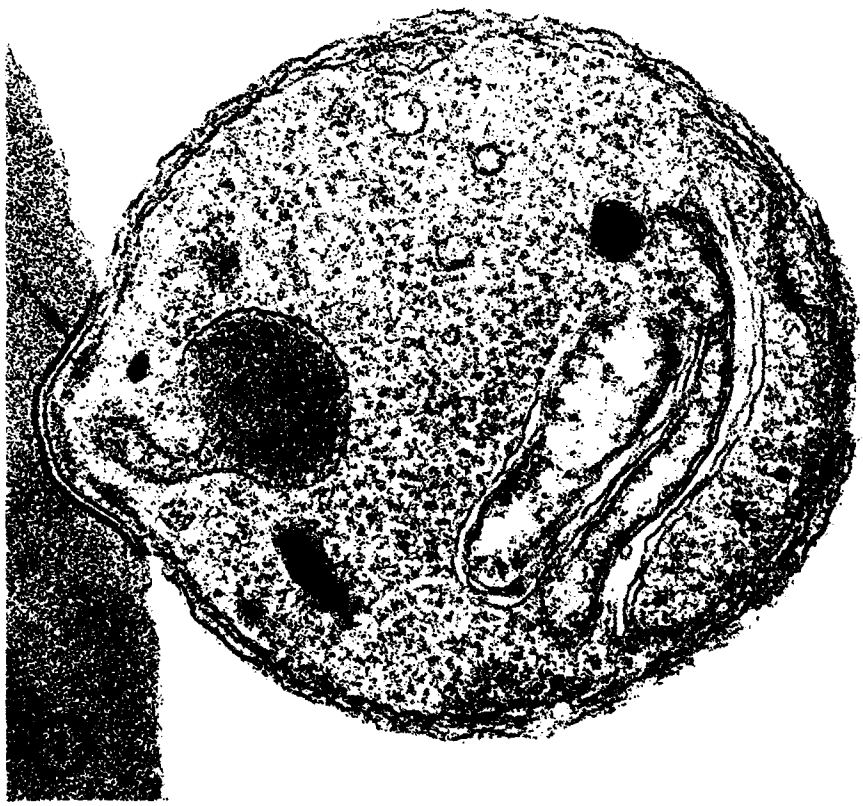

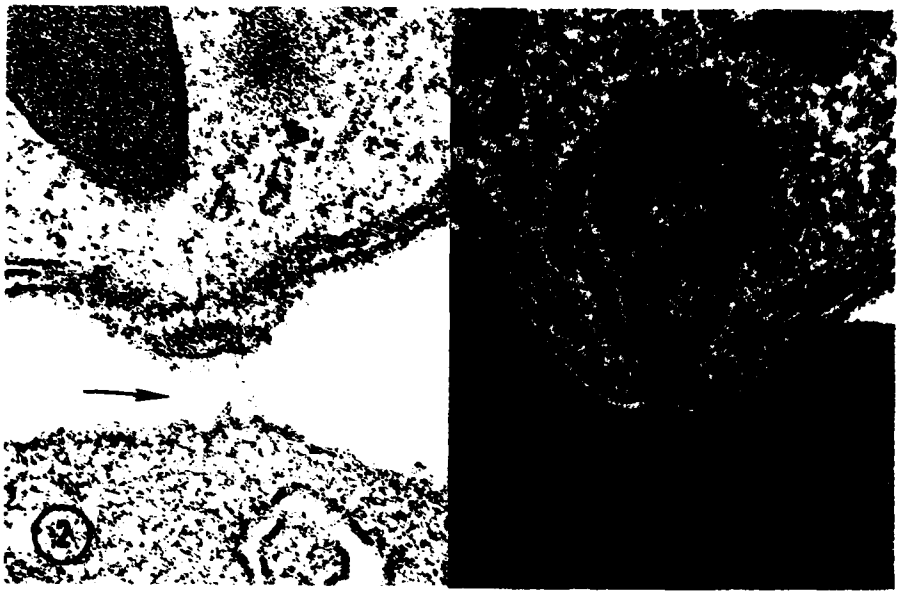

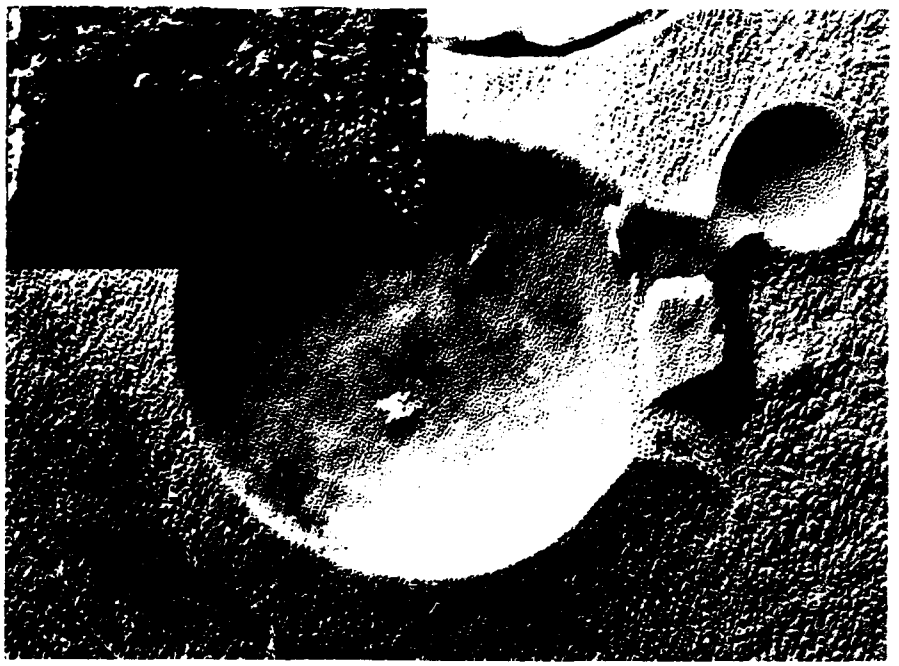

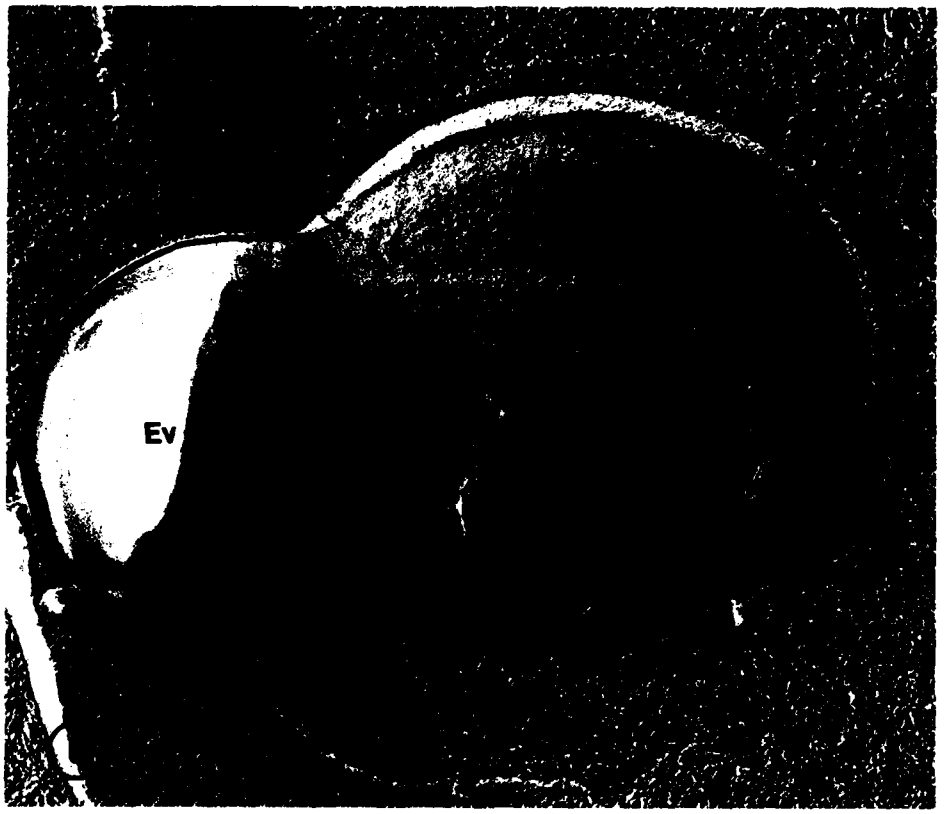
Ev

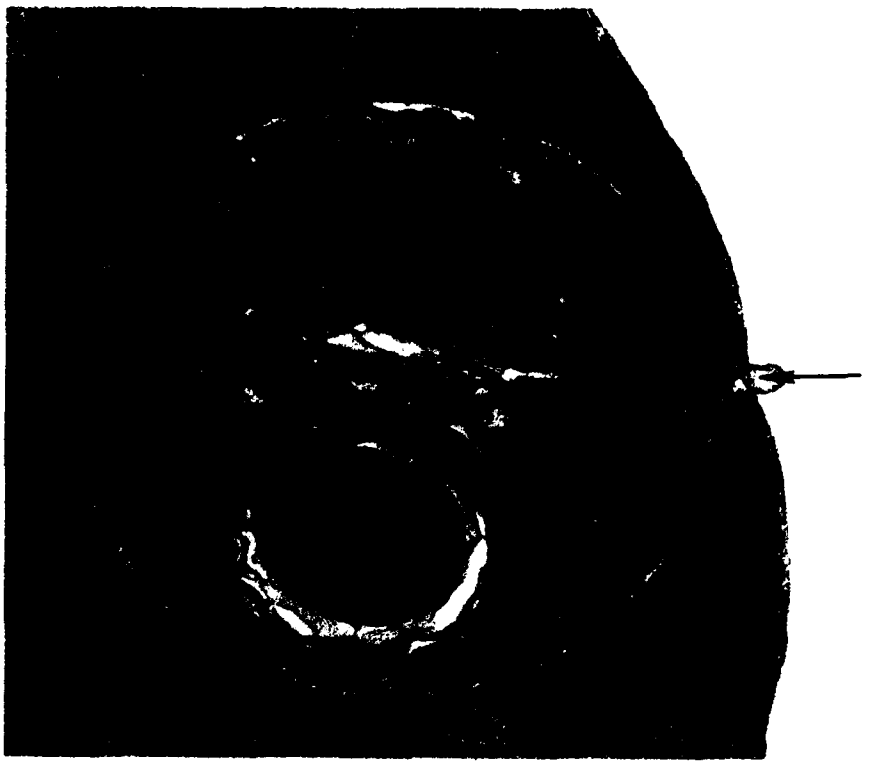

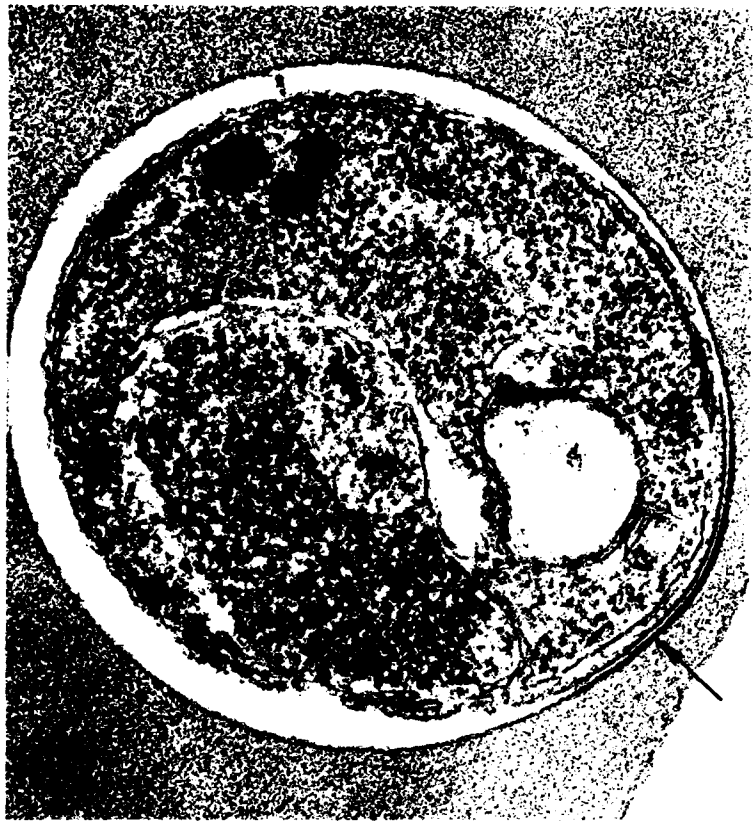

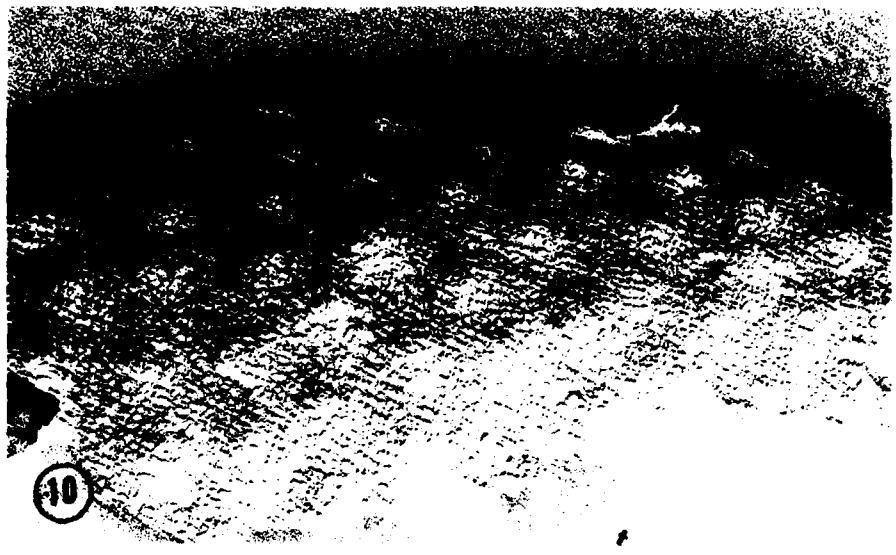
10

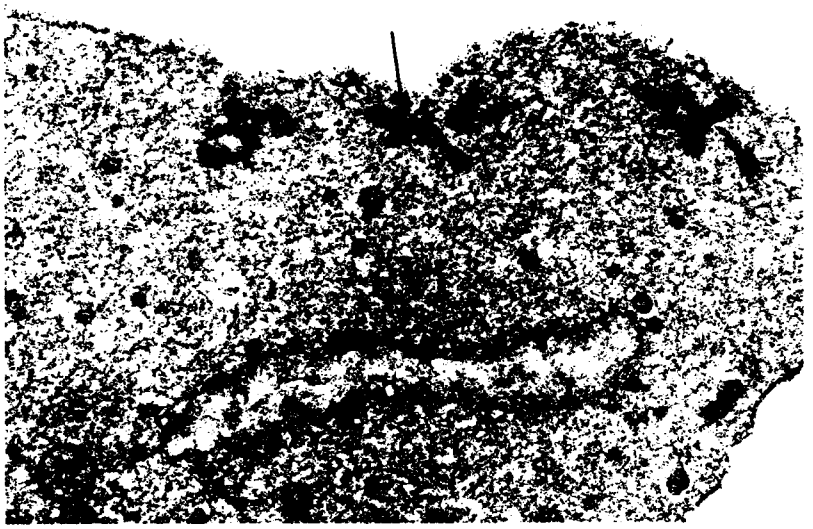

Electron Microscopy of Knobs in P. falciparum Infected Erythrocytes

Masamichi Aikawa[1], John R. Rabbege[1],
Iroka Udeinya[2] and Louis H. Miller[2]

[1] Institute of Pathology, Case Western Reserve University, Cleveland, Ohio 44106

and

[2] Laboratory of Parasitic Diseases, National Institute of Allergy and Infectious Diseases, Bethesda, Maryland 20205

Erythrocytes infected by certain species of malarial parasites show two types of erythrocyte membrane alteration such as electron-dense protrusions called knobs and caveola-vesicle complexes (Aikawa, M. 1977, Bull. WHO, 55:2; Aikawa, M. et al. 1975, Am. J. Path., 79:285). The knobs are found on the membrane of erythrocytes infected with falciparum-type malaria parasites. These knobs form focal junctions with the endothelial cell membranes or with the knobs of other erythrocytes, resulting in the sequestration of these infected erythrocytes along the vascular endothelium (Trager, W. et al. 1966, Bull. WHO, 35:883; Luse, S.A. and Miller, L. H. 1971, Am. J. Trop. Med. Hyg., 20:655; Aikawa, M. et al. 1972, Z. Zellforsch, 124:72; and Udeinya, I. et al., 1981, Science, 213:555). The erythrocyte membrane covering the knobs is immunologically different from the rest of the erythrocyte membrane (Kilejian et al. 1977, Exp. Parasitol., 42:157; Langreth et al. 1979, J. Exp. Med., 150:1241; Chulay, J. et al. 1981, Am. J. Trop. Med. Hyg., 30:12).

The erythrocytes infected with small trophozoites show few knobs, but they increase in number as the parasite grows within the erythrocyte. Because the morphology of these knobs is still not fully understood, we have attempted to characterize them by transmission and scanning electron microscopy together with freeze-fracture and etch techniques.

P. falciparum (Camp strain) in Aotus erythrocytes and P. falciparum (Thailand and Liberian strains) in human erythrocytes were obtained from culture (Udeinya et al. 1981, Science, 213:555). The infected erythrocytes were fixed in 2% glutaraldehyde in 0.1 M cacodylate buffer (pH 7.4) containing 4% sucrose, washed in 0.1 M cacodylate buffer and post-fixed for one hour in 1% osmium tetroxide. After fixation, the samples were centrifuged and then processed for thin section transmission and scanning electron microscopy.

Freeze-fracturing and etching were performed in a Balzers freeze-fracture etching unit. Fracturing was carried out at -120°C under a vacuum of 2×10^{-7} Torr. Etching was performed at -100°C, under a vacuum of 2×10^{-7} Torr for 2 minutes. The surfaces obtained were replicated with platinum and carbon. Replicas were cleaned as described previously (Aikawa, M. et al. 1981, J. Cell. Biol., 91:55). Transmission electron microscopy was performed with a JEOL 100CX electron microscope. Scanning electron microscopy was performed with a JEOL 100CX electron microscope with a scanning unit at 20Kv.

Thin-section electron microscopy showed many knobs on the erythrocytes infected with P. falciparum (Fig. 1). Each knob is a cone-shaped electron-dense structure measuring 30-40nm in height and 90-100nm in width and is covered by the erythrocyte membrane. The base is not sharply demarcated, but gradually merges into the erythrocyte cytoplasm. Scanning electron microscopy showed numerous cone-shaped knobs evenly distributed over the entire erythrocyte surface (Fig. 2). The distribution pattern of the knobs was more easily detectable by scanning electron microscopy than by thin-section transmission electron microscopy. Therefore, scanning electron microscopy appears to be a useful and easy method for the study of knob distribution.

Freeze-fracture and etching demonstrated that the knobs were protruded structures and were evenly distributed over the erythrocyte membrane. The P face of the infected erythrocyte membrane shows evenly distributed intramembrane particles (IMP) and no aggregation or depletion of IMP can be observed over the erythrocyte membrane covering the knobs(Fig. 3). The E face of the infected erythrocyte membrane showed many indentations which correspond to the knobs. Again, no alteration of the IMP distribution can be observed over the knob regions (Fig. 4).

Studies on membrane-membrane interactions such as the membrane fusion between the cells (Loyter et al. 1980, In: Membrane-Membrane Interactions, Raven Press, p. 11) and junction formation (Staehelin 1974, Inter. Rev. Cytol., 39:191) have demonstrated that IMP change their distribution at the site of the interaction. Although our study showed no alteration of IMP distribution on the erythrocyte membrane covering the knobs, it is possible that IMP may change their distribution pattern at the time of the focal junction formation with the endothelial cells. Unaltered IMP distribution on the knob portion of the erythrocyte membrane may correlate with the unaltered surface charge on the erythrocyte membrane covering the knobs induced by P. coatneyi infection (Miller et al. 1972, Exp. Parasitol, 32:86).

Acknowledgements

Supported by NIH grants AI-10645, The U.S. Army R & D Command Contract (DAMD 17-79-C-9029) and WHO (T16/181/M2/52).

Figure Legends

Figures 1-4. Plasmodium falciparum. 1. Transmission electron micrograph of a P. falciparum (Camp strain)-infected erythrocyte showing cone-shaped knobs (arrow) along the erythrocyte membrane. X30,000. Inset: High magnification electron micrograph of an electron-dense knob which is covered by the erythrocyte membrane. X60,000. 2. Scanning electron micrograph of a P. falciparum (Liberian strain)-infected human erythrocyte. Numerous cone-shaped knobs (arrow) are evenly distributed over the entire erythrocyte surface. X40,000. 3. Freeze-fracture and etch replica of a P. falciparum (Thailand strain)-infected human erythrocyte. The P face of the erythrocyte membrane shows evenly distributed IMP and no aggregation or depletion of IMP can be observed over the membrane covering the knobs (arrow). X100,000. 4. Freeze-fracture and etch replica of a P. falciparum (Thailand strain)-infected human erythrocyte. The E face of the erythrocyte membrane shows no changes in IMP distribution over the knobs (arrow). X100,000.

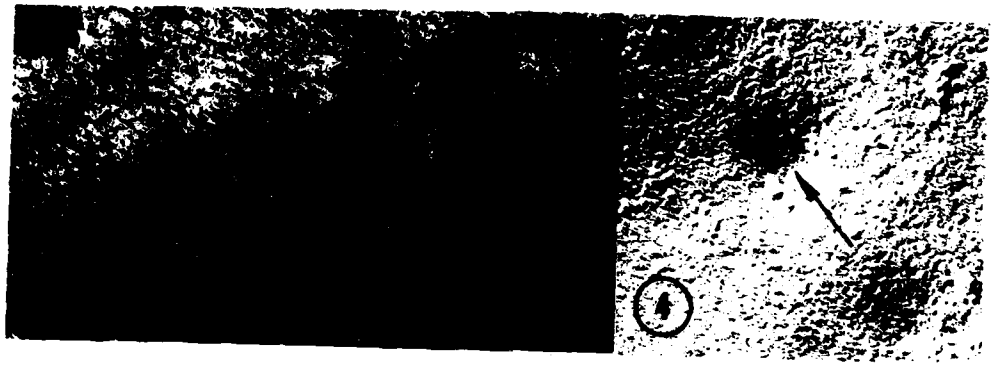

MONOCLONAL ANTIBODIES TO *Trypanosoma cruzi* INHIBIT MOTILITY AND NUCLEIC ACID SYNTHESIS OF CULTURE FORMS

(epimasigotes and metacyclic trypomastigotes)

Running Title: Monoclonal antibodies to T. cruzi culture forms

Maria Julia Manso Alves*, Masamichi Aikawa† and Ruth S. Nussenzweig*

*New York University Medical Center, Department of Microbiology, Division of Parasitology, 550 First Avenue, New York, New York 10016

†Case Western Reserve University, Institute of Pathology Cleveland, Ohio 44106

*Telephone (212) 340-6817

ABSTRACT

Monoclonal antibodies were raised against the surface of epimastigotes and metacyclic trypomastigotes of T. cruzi, as shown by electron microscopy, agglutination and immunofluorescence. The antibodies were stage but not strain-specific. A deleterious effect of the antibodies upon T. cruzi culture forms is shown by the drastic reduction of parasite motility and incorporation of nucleic acid precursors. Some fraction of the parasite population, however, was viable, replicated and infected mouse macrophages in culture. The antibodies were found to also mediate complement-induced lysis of culture forms of T. cruzi.

INTRODUCTION

Circulating antibodies have been detected in humans and animals suffering from Chagas' disease, which is caused by the protozoan flagellate T. cruzi. The role of these antibodies in host resistance to the parasite has been established by passive transfer and by neutralization experiments (reviewed by Brener [3]); however, neither the exact mechanisms nor the antigens involved in this protection have been characterized.

The surface components of T. cruzi have been the focus of a number of recent studies (9) and some of the corresponding antigens have been identified. A major, biochemically well-characterized, surface membrane component of T. cruzi, the lipopeptidophosphoglycan described by Lederkremer et al. (7) was found to be a poor immunogen, posing difficulties for its immunological analysis (2).

Two glycoproteins of approximate molecular weight 75K and 90K appear to be the main parasite components recognized by both human and mouse immune sera (10). The 75K glycoprotein has been detected only in epimastigotes and metacyclic stages, i.e. culture forms. The 90K glycoprotein, according to Snary and Hudson (15), can be detected in all developmental stages of T. cruzi, although the distribution has not been corroborated by others (10). Antibodies raised against the 90K glycoprotein conferred partial protection to mice, and resulted in lower parasitemia and longer survival times upon challenge with blood forms of T. cruzi (15).

Recently, Snary et al (14) using monoclonal antibodies, identified a glycoprotein of 72K present in culture forms. Immunization with this

glycoprotein, purified by affinity chromatography, failed to protect mice against challenge with blood forms.

The fact that some of the main surface antigens recognized by immune sera confer little or no protection against challenge, suggests the possibility that minor antigenic components play an important role in the immune response to T. cruzi. Therefore, the use of hybridoma technology in this system, appears to be a potentially fruitful approach. The present report contains our initial results in this area obtained through the use of monoclonal antibodies.

MATERIALS AND METHODS

Trypanosoma cruzi: The Y strain was isolated from an acute human case of Chagas' disease (13) and the CL strain from a naturally-infected vector (4). Culture cells of T. cruzi were grown in liver infusion-tryptose (Difco Laboratories, Detroit, Michigan) [LIT) medium (5), supplemented with 10% fetal calf serum (Grand Island Biological Co., Grand Island, NY), penicillin (200 µg/ml) and streptomycin (100 units/ml). Metacyclic trypomastigotes were purified from epimastigote forms by chromatography on DE52 resin (1) (Whatman, Ltd., Kent, Great Britain) as follows: 1×10^9 cells were overlayed on a DE52 column (1.5 x 3 cm) and eluted with PBS, pH 7.2. Fractions of 1 ml were collected and followed by optical microscopy. Those fractions containing only trypomastigotes were pooled (≥ 97% trypomastigotes). Blood form trypomastigotes were isolated from Balb/c mice (Timco, Texas Inbred Mice Co., Houston, Texas). The mice were previously irradiated (600 rad) and infected with 5×10^5 blood forms. The trypomastigotes were separated on lymphoprep, as previously described (8). Amastigotes were obtained from culture peritoneal macrophages infected with culture forms of T. cruzi (multiplicity of 1:6).

Monoclonal antibodies: Balb/c mice were immunized every other week by intraperitoneal route with increasing doses of live T. cruzi (1×10^2, 1×10^3, and 1×10^4 culture forms followed by 1×10^5 and 1×10^6 blood forms). Three weeks later, the mice were given an intravenous booster

with 1 x 10^8 sonicated culture forms. The absence of intact parasites was ascertained microscopically. After 4 days, the spleen cells from the boostered mice were fused with P3U1 myeloma line, in the presence of polyethyleneglycol (6). Positive hybridomas were selected by indirect immunofluorescence using glutaraldehyde-fixed cells, cloned by limiting dilution, expanded and injected into pristane-primed CD_2F_1 mice (Cumberland Farms, Clinton, Tennessee) to obtain large quantitites of antibody-rich ascites fluid. The antibodies were partially purified by precipitating ascites fluid or culture supernatants with 50% ammonium sulfate, followed by chromatography in Sephadex G-200 (Pharmacia Fine Chemicals, Piscataway, NJ). The antibody class was determined by double diffusion in agar using supernatants of cultures (10 x concentrated by 50% ammonium sulfate) against specific antisera for mouse immunoglobulin subtypes (Litton Bionetics, Kensington, Md).

Effect of the monoclonal antibodies on the synthesis of nucleic acids by T. cruzi: For each experimental point, 1 x 10^7 culture cells, in 0.5 ml of LIT Medium or LIT medium containing monoclonal antibodies, were incubated at 28°C for 4, 8, 24 or 120 hours. The monoclonal antibodies were used at a concentration of 500 or 50 µg protein/ml. After the corresponding incubation time, the cells were washed with PBS and resuspended in Dulbecco's Modified Eagle Medium (DMEM) (GIBCO, Grand Island, NY) containing 2 uCi/ml of [5, 6^3H]-uridine or (Methyl-[^{3}H]-thymidine (New England Nuclear, Boston, Mass.), 10% fetal calf serum, penicillin (200 µg/ml)and streptomycin (100 units/ml). After three hours at 28°C, the cells were centrifuged, and the radioactivity precipitated by 5% trichloroacetic acid determined in a liquid scintillation counter.

The same experiment was done with DMEM instead of LIT medium. All experiments were done in duplicate. Anti-P. falciparum monoclonal antibody (2C11) was used as a control, as well as medium alone. Under the conditions described, the incorporation of [^{3}H]-uridine and [^{3}H]-thymidine was proportional to the number of T. cruzi culture cells present (approximately 1 x 10^7 to 4 x 10^7 cells).

Agglutination assay: Culture cells of T. cruzi were washed 3 times with PBS and resuspended in the same buffer. 5 x 10^5/ml were incubated with monoclonal antibodies for 30 min at room temperature and the agglutination followed microscopically. Unrelated monoclonals (anti-P. cynomolgi and anti-P. berghei sporozoites) were used as controls.

T. cruzi lysis: T. cruzi cells were labeled with [^{3}H]-uridine as described above and washed with PBS (3x). 3 x 10^5 labeled cells were incubated in 50 µl of PBS or PBS upon addition of monoclonal antibodies at the desired concentration. After 1 hr at 28°C, fresh or heat inactivated human serum (56°C, 1 hr) was added to a final concentration of 10% and incubated for an another 30 min at 28°C. The cells were then spun down (1000 g, 15') and 30 µl of the supernatant fluid was counted in a liquid scintillation counter. The percentage of lysed cells was related to the radioactivity released by the same amount of cells treated with 1% Nonidet P-40 (20 min at room temperature) and taken as 100%.

Macrophage infection by T. cruzi: Marrow-derived macrophages were obtained by seeding 5 x 10^5 bone marrow cells per 12 mm diameter coverglasses

and distributed in 16 mm diameter Costar plates, as described earlier (11). 1×10^6 culture forms of T. cruzi were treated with 500 g/ml of monoclonal antibody or with LIT medium for 1, 48 or 96 hours at which time the cells were incubated with the macrophages. The free parasites were removed by three washes with culture medium and the macrophages were incubated for an additional 24 hrs. The cells were then fixed in methanol and stained with Giemsa. The macrophages containing three or more intracellular parasites were scored as infected. At least 200 macrophages were scored per coverglass. Duplicate determinations were used for each incubation time.

Electron Microscopy: T. cruzi was incubated with serum from mice bearing the myeloma tumour for 1 hr at room temperature, washed and fixed in 2.5% glutaraldehyde, 0.1 M cacodylate buffer, pH 7.3, and 4% sucrose. The preparation was post-fixed in 1% osmium tetroxide for 1 hr, dehydrated, and then embedded in Epon 812. The sections were examined with a Siemens Elmiskop 101 electron microscope.

RESULTS

We selected eleven hybridomas based on their reactivity with glutaraldehyde-fixed T. cruzi in an indirect immunofluorescence assay. These hybridomas were cloned, and all were found to react with both culture forms, i.e. epimastigotes and metacyclic stages of T. cruzi. Several of these monoclonals incubated with unfixed, viable culture stages, were found to produce immunofluorescence of the parasite's membrane and agglutination of the cells.

Two hybridomas (B10/1 and B2/5) were chosen for more extensive characterization. They were characterized as being of the IgG1 and IgG3 subclasses, respectively, with κ light chains. The two monoclonals produced the same pattern of uniform membrane fluorescence with glutaraldehyde-fixed epimastigotes and trypomastigotes of both the Y and CL strains of T. cruzi. Under identical conditions, however, both the monoclonals failed to react with either amastigotes or blood forms of these two parasite strains (Table 1). A certain variability in the fluorescent staining of individual culture forms was detected when viable cells were incubated with the monoclonal antibodies.

The incubation of live culture forms of T. cruzi with monoclonals B10/1 and B2/5 was found to result in strong agglutination of both trypomastigotes and epimastigotes, as well as its intermediate forms (Figure 1). Agglutination of culture forms (5×10^5) was observed upon incubation of the cells with ≥ 10 μg/ml of the purified monoclonals. Incubation of the parasites with higher concentrations of these monoclonals

($\geq$ 200 μg/ml) resulted almost immediately in a drastic reduction of parasite motility. In fact, most of the parasites rapidly became immobilized, interfering with clump formation. This interaction is stage-and species-specific; it did not occur upon incubation of the monoclonals with blood forms of T. cruzi or with promastigotes of Leishmania mexicana amazonensis. Unrelated monoclonals (anti-P. berghei and anti-P. cynomolgi), failed to induce immobilization, agglutination or immunofluorescence of epimastigotes or trypomastigotes of T. cruzi under identical experimental conditions.

In an attempt to identify the mechanism of interaction of monoclonal antibodies with parasites, we investigated the long-term effects of these antibodies on the nucleic acid synthesis by culture forms of T. cruzi. Parasites (1×10^7 cells) were incubated for variable time periods with either 50 or 500 μg/ml of B10/1 or B2/5. As controls, an equal number of parasites were incubated with the culture medium (LIT) alone, or upon addition of an unrelated monoclonal (2C11). The parasites were then washed, and incubated with either [^{3}H]-thymidine or [^{3}H]-uridine for 3 hours. The radioactivity incorporated under these conditions was measured in the corresponding TCA precipitates (Figure 2). The values obtained for both controls, i.e., parasites incubated in medium alone, or upon addition of an unrelated monoclonal, were very similar. Both hybridomas (B10/1 and B2/5) were strongly inhibitory, significantly reducing the uridine and thymidine incorporation of the parasites as compared to the controls. There were quantitative differences, however, in the effects produced by these two monoclonals. At equivalent concentrations B2/5 was more active. When T. cruzi was

incubated with the monoclonals for 4-8 hours the inhibitory effect was clearly detected by measuring uridine incorporation. A drastic reduction of incorporation of both precursors was seen after 24 and 48 hours of incubation with either one of the hybridomas. During this period, we observed the occurrence of large numbers of non-motile, apparently non-viable parasites. Determination of the percentage of non-viable culture forms was however unfeasible in view of extensive antibody-induced agglutination. After five days of incubation in the presence of monoclonals, some of the parasites appeared to escape this inhibitory effect, indicating the presence of a viable parasite population.

The persistence of viable, infective culture forms upon incubation of the parasites with the monoclonals was also confirmed by exposing cultured mouse macrophages to antibody-treated parasites. Preincubation of the parasites with 500 µg/ml of monoclonal B10/1 for 1 hr, 48 hrs or 96 hrs, resulted in 80%, 36% and 50% infected macrophages, respectively.

In a different set of experiments in which the parasites and monoclonals (B10/1 or B2/5) were incubated simultaneously with macrophages, parasite interiorization was enhanced, as compared with the controls. The intracellular development appeared to be unaltered. After 3-4 days, however, we noted the complete absence of free epimastigotes in the surrounding culture medium, as if parasite development had been arrested at the amastigote stage due to the presence of the monoclonal. This was in direct contrast to the occurrence observed in control cultures in which epimastigotes were abundant at this time.

Both monoclonals, B2/5 and B10/1, were found to mediate complement-induced lysis of culture forms of T. cruzi (Table 2). Since the epi-

mastigotes are lysed by complement in the absence of antibody, the experiment was done at 28°C rather than the standard 37°C to minimize these effects. Complement activation appears to be mediated by the alternative pathway, since it is inhibited by 1mM EDTA, but remains unaltered in the presence of 1mM EGTA and 3mM $MgCl_2$. Under these experimental conditions, even upon incubation with high concentrations of antibodies, lysis was never complete. This indicates the presence of a relatively more resistant parasite population which may correspond to a particular developmental stage.

DISCUSSION

Several of the antibodies we obtained were directed against T. cruzi surface antigens. These antibodies reacted not only with glutaraldehyde-fixed parasites, but also bound, agglutinated and immobilized viable culture forms. Agglutination and immobilization of T. cruzi was not reported to occur in a recent paper on this subject, which also involved the use of hybridoma methodology (14). This may either be due to different specificities and/or differences in the binding affinity and isotype of the respective antibodies. In the present experiments, the mice used for fusion were immunized with intact, viable parasites. This immunization procedure makes it difficult to obtain spleen cells and hybrids free of live T. cruzi. However, immunization with dead parasites resulted in lower antibody titers.

Our results indicate that monoclonals against T. cruzi distinguish stage-specific antigens, and might provide useful markers to separate this parasite from other related hemoflagellates. While these monoclonals cannot distinguish between Y and CL strains, extension of the work to other T. cruzi strains appears desirable.

With regard to the stage specificity of T. cruzi, an important, yet unanswered question concerns the reactivity of our monoclonals with the metacyclic infective forms found in triatomes. It is likely that in the identification of functional antigens, the infective forms are of greatest interest and crucial proof of protection ought to be resistance to challenge with metacyclic insect stages.

The properties of the two monoclonals appeared qualitatively similar. Differences in antibody titers or in inhibitory effects on motility and metabolism may depend on different binding affinities. However, conclusions as to the specificity of the antibodies have to await the characterization of the relevant antigens.

Prolonged incubation of the parasites with the specific monoclonal antibodies was required to detect inhibitory activity on parasite metabolism and replication in cell-free cultures, as well as decrease of the percentage of infected macrophages. The results were identical whether we used LIT or DMEM medium, or whether the fetal calf serum had or had not been heat-inactivated, thereby indicating that this inactivation was not complement-mediated nor determined by the presence of a particular component of the culture media.

The inhibitory effect of the monoclonal antibodies upon nucleic acid synthesis of T. cruzi is partial. The same partial effect was also observed in macrophage-parasite interaction and in antibody-induced, complement-mediated lysis. Although different mechanisms might cause these interactions, the presence of viable parasites upon prolonged incubation with antibody might have one common explanation. Since we worked with a heterogeneous, non-cloned, asynchronous parasite population, our results could be explained if a fraction of the population was genetically distinct. Under these conditions, some of the parasites could either lack or express only minimal amounts of the relevant surface antigen which is present on the remaining population. Alternatively, if the antigen in question is expressed only on a well-defined developmental stage, this might also explain our results. Another hypothesis is that

different parasite populations might have different rates of removal of antigen and/or antigen/antibody complexes from their surfaces. Isolation of the parasites resistant to the effect of monoclonals might enable us to distinguish more easily between these different "escape" mechanisms.

Much of the deleterious effect of the monoclonals on the parasites might be due to membrane cross-linking and agglutination. In fact, we found that the F(ab) fragments of both monoclonals failed to agglutinate and to inhibit uridine and thymidine incorporation by T. cruzi [not shown.]

Finally, the failure of these antibodies to affect the entire parasite population may explain the parasitemia and death of mice inoculated with antibody-treated cultures of T. cruzi [not shown.] Taken together, these results indicate that although protective antigen(s) of T. cruzi still remain unidentified, these as well as other monoclonals will contribute to the delineation of the antigenic repertoire of the parasite, and the mechanism(s) of the interaction of the antibody with the parasite.

ACKNOWLEDGMENTS

This work was supported by the UNDP/World Bank/WHO Special Programme for Research and Training in Tropical Diseases (TIG/181/T8/31 and U.S. Army R& D Command DAMD17-79-C-9029. Dr. M.J.M. Alves was a recepient of fellowships from FAPESP and CNPq, Brasil during this research period.

TABLE I. STAGE AND STRAIN SPECIFICITY OF THE T. cruzi SURFACE ANTIGEN RECOGNIZED BY MONOCLONAL B10/1 DETERMINED BY IMMUNOFLUORESENCE

Glutaraldehyde-fixed* Parasites	T. cruzi Strain	IFA Titer**
Epimastigote	Y	1:160
Metacylic	Y	1:320
Amastigote	Y	NEG
Blood Forms	Y	NEG
Epimastigote	CL	1:80
Metacylic	CL	1:80
Blood Forms	CL	NEG

* Parasites were fixed with 0.2% glutaraldehyde in 0.1 M cacodylate buffer pH 7.2 for 20 min at room temperature.

**The monoclonal antibody used in these reactions (B10/1) was partially purified by precipitation with 50% amnonium sulfate.

TABLE II. HYBRIDOMA-MEDIATED COMPLEMENT DEPENDENT LYSIS OF CULTURE FORMS OF *T. cruzi*[*]

Monoclonal	µg/ml	% Lysis[**] Metacylic trypomastigotes HuS[***]	Metacylic trypomastigotes IHuS[***]	Epimastigotes HuS[***]	Epimastigotes IHuS[***]
-	-	15	8	26	25
B2/5	500	87	14	40	23
	50	76	15	33	27
	5	42	19	27	24
B10/1	500	78	17	65	37
	50	30	18	57	27
	5	28	17	45	28
2C11[****]	500	25	28	27	24

* Parasites were metabolically labeled with [^{3}H]-uridine for 3 hrs at 28°C.

** 100% lysis corresponds to the radioactivity released by parasites incubated with 1% NP-40.

*** HuS (human serum); IHuS (heat-inactivated human serum).

**** anti-*P. falciparum* hybridoma

Figure 1

Figure 1a Light micrograph of the culture forms of T. cruzi incubated with hybridoma-derived monoclonal (B2/5) Bar indicates 10 μ

Figure 1b Electron micrograph of the metacyclic trypomastigotes of T. cruzi incubated with hybridoma-derived monoclonal (B2/5). Note agglutination of the parasite [arrow] Bar indicates 1.5 μ (Inset): Higher magnification micrograph showing fibrillar structure which adheres to these parasites Bar indicates 0.1 μ

Figure 1c Electron micrograph of the metacyclic trypomastigotes of T. cruzi incubated with anti-P. knowlesi antibody. No agglutination takes place between the parasites. Bar indicates 0.25 μ


1a
1b

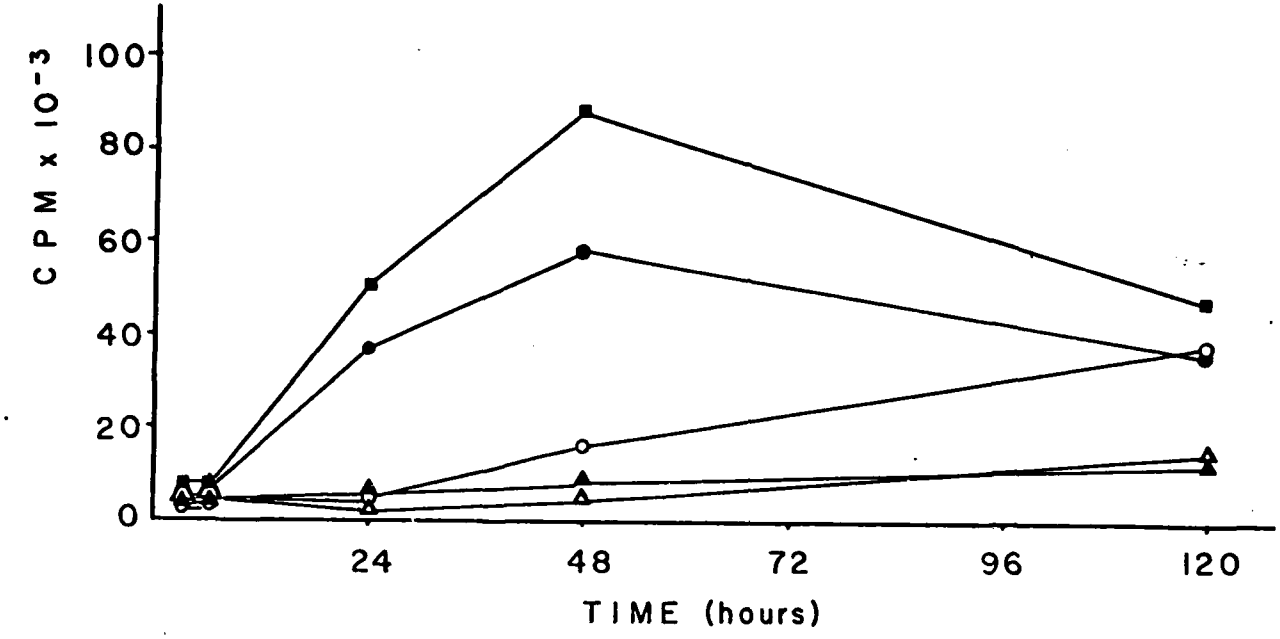
CPM x 10⁻³
100
80
60
40
20
0
24
48
72
96
120
TIME (hours)

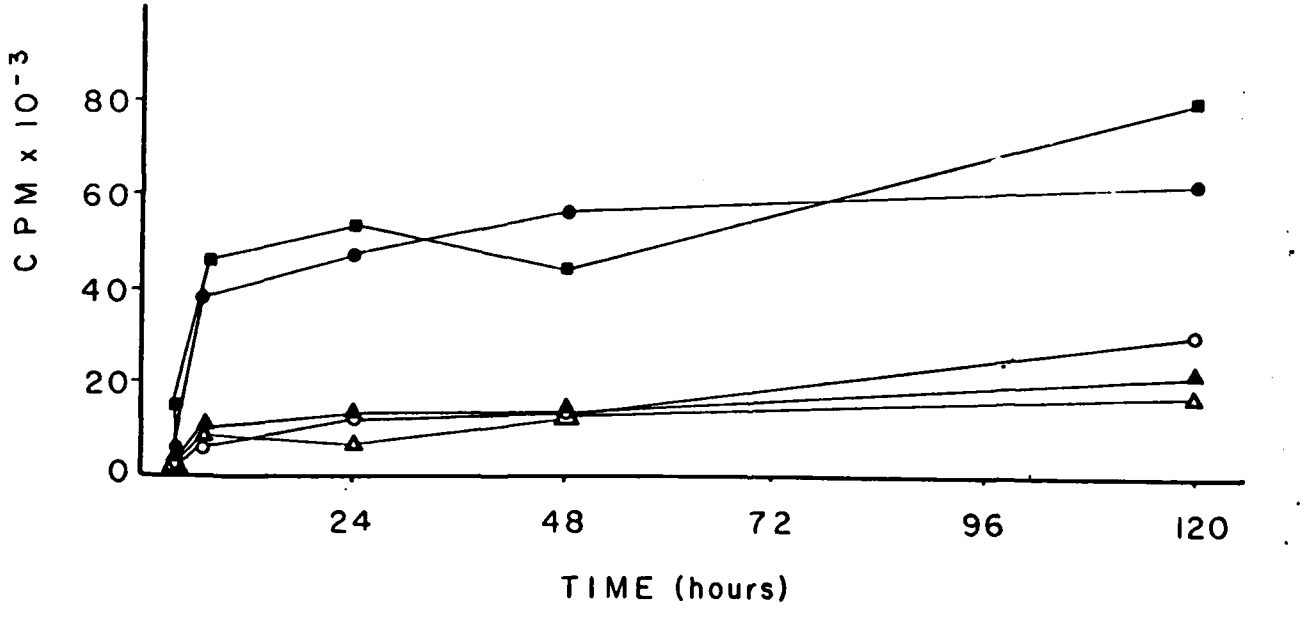
CPM x 10⁻³
80
60
40
20
0
24
48
72
96
120
TIME (hours)

Figure 2 Incorporation of [^{3}H]-thymidine and [^{3}H]-uridine by culture forms of T. cruzi pre-incubated with monoclonal antibodies (B10/1 or B2/5) or control medium. Abscissa: period of incubation with antibodies or control medium. Ordinates: Radioisotope incorporation in TCA precipitates (cpm). Radioactive precursors were given 3 hrs following incubation with antibodies. Upper graph: [^{3}H]-thymidine; Lower graph: [^{3}H]-uridine.

▨ LIT medium; ▲ B2/5, 500 µg/ml; △ B2/5, 50 µg/ml;

○ B10/1, 500 µg/ml ● B10/1, 50 µg/ml

AD-A136 754 ELECTRON MICROSCOPY OF INTRACELLULAR PROTOZOA(U) CASE WESTERN RESERVE UNIV CLEVELAND OHIO INST OF PATHOLOGY M AIKAWA AUG 82 DAMD17-79-C-9029 2/2

UNCLASSIFIED F/G 6/5 NL

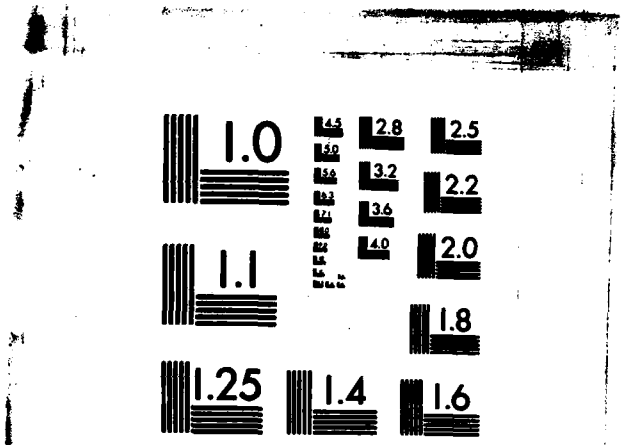

LITERATURE CITED

1. Al-Abbassy, S.N., T.M. Scod and J.P. Kreier. 1972. Isolation of the trypomastigote form of Trypanosoma cruzi from a mixture of the trypomastigote and epimastigote forms of the parasite by use of a DEAE-cellulose column. J. Parasitol. 58: 631-632.
2. Alves, M.J.M., J.F. da Silveira, C.H.R. de Paiva, C.T. Tanaka and W. Colli. 1979. Evidence for the plasma membrane localization of carbohydrate-containing macromolecules from epimastigote forms of Trypanosoma cruzi. FEBS Lett. 99: 81-85.
3. Brener, Z. 1980. Immunity to Trypanosoma cruzi. Adv. Parasitol. 18: 247-292.
4. Brener, Z. and E. Chiari. 1963. Variaçoẽs morfologicas observadas em diferentes amostras de Trypanosoma cruzi. Rev. Inst. Med. Trop. Sao Paulo. 5: 220-224.
5. Camargo, E.P. 1964. Growth and differentiation in Trypanosoma cruzi. I. Origin of metacyclic trypanosomes in liquid media. Rev. Inst. Med. Trop. Sao Paulo. 6: 93-100.
6. Köhler, G. and C. Milstein. 1975. Continuous cultures of fused cells secreting antibody of predefined specificity. Nature (London) 256: 495-498.
7. Lederkremer, R.M., M.J.M. Alves, G.C. Fonseca and W. Colli. 1976. A lipopeptidophosphoglycan from Trypanosoma cruzi (epimastigote). Isolation, purification and carbohydrate composition. Biochim. Biophys. Acta 44: 85-89.
8. Mercado, T.I. and K. Katusha. 1979. Isolation of Trypanosoma cruzi from the blood of infected mice by column chromatography.

Prep. Biochem. 9: 97-106.

9. Mitchell, G.F. and R.F. Anders. 1982. Parasite antigens and their immunogenicity in infected hosts. p. 70-149. In M. Sela (ed.), The Antigens VI, Academic Press, Inc., New York

10. Nogueira, N., S. Chaplan, J.D. Tydings, J. Unkeless and Z. Cohn. 1981. Trypanosoma cruzi. Surface antigens of blood and culture forms. J. Exp. Med. 153: 629-639.

11. Rabinovitch, M., J.P. Dedet, A. Ryter, R. Robineaux, G. Topper and E. Brunet. 1982. Destruction of Leishmania mexicana amazonensis amastigotes within macrophages in culture by phenazine methosulfate and other electron carriers. J. Exp. Med. 155: 415-431.

12. Scott, M.T. and D. Snary. 1979. Protective immunization of mice using cell surface glycoprotein from Trypanosoma cruzi. Nature (London) 282: 73-76.

13. Silva, L.H.P. and V. Nussenzweig. 1953. Sobre uma cepa de Trypanosoma cruzi altamente virulenta para o camundongo branco. Folia Clin. Biol. 20: 191-208.

14. Snary, D., M.A.J. Ferguson, M.T. Scott and A.K. Allen. 1981. Cell surface antigens of Trypanosoma cruzi: Use of monoclonal antibodies to identify and isolate an epimastigote specific glycoprotein. Molec. Biochem. Parasitol. 3: 343-356.

15. Snary, D. and L. Hudson 1979. Trypanosoma cruzi cell surface proteins: identification of one major glycoprotein. FEBS Lett. 100: 166-170.

3. Update Bibliography of Published Works

a. Aikawa, M., Miller, L.H., Rabbege, J.R. and Epstein, N., Freeze-fracture study on the erythrocyte membrane during malarial parasite invasion. J. Cell Biol. 91:55-62, 1981.

b. Ito, Y., Furuya, M., Oka, M., Ozaki, H. and Aikawa, M., Transmission and scanning electron microscopic study of micronemata of Trypanosoma gambiease, J. Protozool. 28:313-316, 1981.

c. Aikawa, M., Rener, J., Carter, R. and Miller, L.H., An electron microscopic study of the interaction of monoclonal antibodies with gametes of the malarial parasites, Plasmodium gallinaceum. J. Protozool. 28:383-388, 1981.

d. Aikawa, M., Hendricks, L.D., Ito, Y. and Jagusiak, M., Interactions between macrophage-like cells and Leishmania brasiliensis in vitro. Am. J. Path. (In Press), 1982.

e. Aikawa, M., Rabbege, J.R., Udeinya, I. and Miller, L.H., Electron microscopy of knobs in P. falciparum infected erythrocytes. J. Parasitol. (In Press), 1982.

f. Aikawa, M., Fine structure of malarial parasites in the various stages of development. In: Textbook of Malaria. (ed. by Wernsdorfer, W.H. and McGregor, I.A.) Churchill Livingstone, London, (In Press), 1982.

g. Aikawa, M., Host-parasite interaction: Electron microscopic study. In: The Molecular Biology of Parasites (ed. by L. Luzzato and J. Guardiola), Raven Press, London, (In Press), 1982.

h. Aikawa, M. and Miller, L.H. Structural alteration of erythrocyte membrane during malarial parasite invasion. In: Ciba Foundation Symposia on Malaria and the Red Cell. (ed. by Dr. Evered), Ciba Foundation, London, (In Press), 1982.

i. Alves, J.M., Aikawa, M. and Nussenzweig, R.S., Monoclonal Antibodies to Trypanosoma cruzi inhibit motility and nucleic acid aynthesis of cultured forms. (Submitted for publication), 1982.

12 Copies	Director (Attn: SGRD-UWZ-AG) Walter Reed Army Institute of Research Walter Reed Army Medical Center Washington, D.C. 20012
4 Copies	HGDA (SGRD-SI) Fort Detrick Frederick, MD 21701
12 Copies	Defense Documentaion Center Attn: DDC-DCA Cameron Station Alexandria, Virginia 22314
1 Copy	Dean School of Medicine Uniformed Services University of Health Sciences 4301 Jones Bridge Road Bethesda, Maryland 20014
1 Copy	Superintendent Academy of Health Sciences U.S. Army Attn: AHS-COM Fort Sam Houston, Texas 78234

END

FILMED

2-84

DTIC